A novel arousal-based individual screening reveals susceptibility and resilience to PTSD-like phenotypes in mice

Sebastiano A. Torrisi [a], Gianluca Lavanco [a,b,1], Oriana M. Maurel [a,c,1], Walter Gulisano [a], Samuele Laudani [a], Federica Geraci [a], Margherita Grasso [d,e], Cristina Barbagallo [a], Filippo Caraci [d,e], Claudio Bucolo [a], Marco Ragusa [a,d], Francesco Papaleo [f], Patrizia Campolongo [g,h], Daniela Puzzo [a], Filippo Drago [a], Salvatore Salomone [a,1], Gian Marco Leggio [a,*,2]

[a] Department of Biomedical and Biotechnological Sciences, University of Catania, Catania, Italy
[b] INSERM, U1215 Neurocentre Magendie and University of Bordeaux, Bordeaux, France
[c] Research Group "Neuronal Plasticity", Max Planck Institute of Psychiatry, Munich, Germany
[d] Oasi Research Institute-IRCCS, Troina, Italy
[e] Department of Drug Sciences, University of Catania, Catania, Italy
[f] Genetics of Cognition Laboratory, Neuroscience area, Istituto Italiano di Tecnologia, Genova, Italy
[g] Department of Physiology and Pharmacology "Vittorio Erspamer", Sapienza University of Rome, Rome, Italy
[h] Neurobiology of Behavior Laboratory, Santa Lucia Foundation, Rome, Italy

ARTICLE INFO

ABSTRACT

Translational animal models for studying post-traumatic stress disorder (PTSD) are valuable for elucidating the poorly understood neurobiology of this neuropsychiatric disorder. These models should encompass crucial features, including persistence of PTSD-like phenotypes triggered after exposure to a single traumatic event, trauma susceptibility/resilience and predictive validity. Here we propose a novel arousal-based individual screening (AIS) model that recapitulates all these features. The AIS model was designed by coupling the traumatization (24 h restraint) of C57BL/6 J mice with a novel individual screening. This screening consists of z-normalization of post-trauma changes in startle reactivity, which is a measure of arousal depending on neural circuits conserved across mammals. Through the AIS model, we identified susceptible mice showing long-lasting hyperarousal (up to 56 days post-trauma), and resilient mice showing normal arousal. Susceptible mice further showed persistent PTSD-like phenotypes including exaggerated fear reactivity and avoidance of trauma-related cue (up to 75 days post-trauma), increased avoidance-like behavior and social/cognitive impairment. Conversely, resilient mice adopted active coping strategies, behaving like control mice. We further uncovered novel transcriptional signatures driven by PTSD-related genes as well as dysfunction of hypothalamic–pituitary–adrenal axis, which corroborated the segregation in susceptible/resilient subpopulations obtained through the AIS model and correlated with trauma susceptibility/resilience. Impaired hippocampal synaptic plasticity was also observed in susceptible mice. Finally, chronic treatment with paroxetine ameliorated the PTSD-like phenotypes of susceptible mice. These findings indicate that the AIS model might be a new translational animal model for the study of crucial features of PTSD. It might shed light on the unclear PTSD neurobiology and identify new pharmacological targets for this difficult-to-treat disorder.

1. Introduction

Post-traumatic stress disorder (PTSD) is a neuropsychiatric disorder developed by vulnerable individuals following a traumatic event. PTSD is considered a major health challenge (Shalev et al., 2017). The suicide risk associated with PTSD is very high (Kessler, 2000) and available treatments with the selective serotonin reuptake inhibitors (SSRIs) paroxetine and sertraline, which are the only two medications approved by U.S. Food and Drug Administration (FDA), are unsatisfactory (Malikowska-Racia and Salat, 2019; Torrisi et al., 2019). Thus, there is an urgent need to develop more effective treatments for PTSD. To this purpose, animal models are recognized essential tools for studying human diseases as well as for screening and identify new potential drugs (Berardi et al., 2016; Everitt et al., 2018). Although available animal models for the study of PTSD have provided important insights, new models with a high translational value may be however useful. Indeed, several reports have outlined challenges that need to be addressed to shape a useful animal model for the study of PTSD (Berardi et al., 2014; Daskalakis et al., 2013; Deslauriers et al., 2018; Hendriksen et al., 2014; Richter-Levin et al., 2019). Because PTSD is often triggered by exposure to a single traumatic event (Musazzi et al., 2018), a single/acute traumatic procedure should be used rather than repeated/chronic stressful procedures, in order to trigger phenotypes closer to PTSD and diminish the probability of producing depressive-like phenotypes (Siegmund and Wotjak, 2006). The persistence of several behavioral phenotypes resembling PTSD symptoms, which are not only fear-related, is highly required for two reasons. First, according to criterion F for PTSD diagnosis of the Diagnostic and Statistical Manual of Mental Disorders (DSM-5), symptoms must last for more than one month (American Psychiatric Association DSM-5 Task Force, 2013). Second, whereas some individuals with PTSD recover soon after the diagnosis, many others can suffer from PTSD for several months or years (American Psychiatric Association DSM-5 Task Force, 2013; Kessler et al., 1995). More importantly, the long-term manifestation of susceptibility and resilience to the trauma is of high relevance for face validity of animal models (Richter-Levin et al., 2019; Sillivan et al., 2017). In this regard, some available models classify animals in susceptible and resilient (Cohen et al., 2004; Olson et al., 2011; Sillivan et al., 2017). However, in an experimental model is very difficult to reproduce the clinical evidence that only a subset of humans who experience a "traumatic event" are prone to develop PTSD (Hendriksen et al., 2014; Sillivan et al., 2017; Zhang et al., 2019). At the molecular level, it would be useful in a PTSD animal model, to have an overlapping with human findings showing biological changes in individuals with PTSD. Furthermore, useful animal models for the study of PTSD should include the predictive validity criterion, i.e. the prediction of treatment effects in individuals with PTSD on the basis of treatment effects on PTSD-like phenotypes observed in rodents (Hendriksen et al., 2014; Richter-Levin et al., 2019; Zhang et al., 2019). In an attempt to address altogether these challenges, we developed a novel arousal-based individual screening (AIS) model for the study of PTSD. To shape this model, we combined the traumatization of C57BL/6 J mice with a novel individual screening relying on long-term z-normalization of change in post-trauma acoustic startle reactivity (ASR), which is a well-validated measure of arousal depending on neural circuits conserved across mammals (Bale et al., 2019). Through the AIS model, we provide evidence that mice exposed to 24 h of restraint, which is a single, long and severe traumatic procedure (Chu et al., 2016), can be segregated in susceptible and resilient subpopulations according to an "arousal score" obtained through the z-normalization. Interestingly, susceptible and resilient mice identified through the AIS model showed long lasting and persistent behavioral correlates of PTSD symptoms when tested in a battery of experimental paradigms. To support the validity of the segregation in subpopulations, several molecular and electrophysiological analyses were carried out. Moreover, mice were chronically treated with paroxetine to evaluate the predictive validity of this animal model. Because different

complementary symptoms fluctuating over time characterize PTSD, we further applied the z-normalization to all behavioral tests in order to create composite scores for each behavioral dimension. Finally, we created a comprehensive "PTSD-like score", a single value originating from all the other scores. This PTSD-like score provided a general overview of the phenotypes as well as a general overview of the pre-clinical effects of paroxetine.

2. Materials and methods

Details regarding the AIS model, behavioral experiments [odor-cued fear conditioning test, open field (OF) test, elevated plus maze (EPM) test, 5-trial social memory (5-trial SM) test, forced swim test (FST)], analysis of gene expression and electrophysiological recordings are provided in supplementary materials and methods.

2.1. Animals

Male C57BL6/J mice (total n = 200, 8–16 weeks old at the beginning of the experiments, Charles River Laboratories Italia, Italy) were group-housed 3–5 per cage under controlled conditions (12-h light/dark cycle, $22 \pm 2\,°C$, food and water ad libitum) and weighed once a week until the end of each experimental protocol. The experimenter handled animals on alternate days during the week preceding the stress procedure. Animals were acclimatized to the testing room at least 1 h before the beginning of the tests. All experiments were carried out according to EU Directive 2010/63/EU, the Institutional Animal Care and Use Committees of Catania and the Italian Ministry of Health (authorization n.110/2019 PR).

2.2. Experimental design

2.2.1. Experiment 1: the arousal-based individual screening (AIS) model

Hyperarousal symptoms, including exaggerated startle reactivity and hypervigilance, are core symptoms of PTSD [criterion E, DSM-5; (American Psychiatric Association DSM-5 Task Force, 2013)]. They regularly occur early (Bremner et al., 1996) and have a major impact in the natural course of the disease, further influencing the development of other symptoms (Morena et al., 2015; Schell et al., 2004). For these reasons, here post-trauma changes of ASR were measured to detect hyperarousal (Fig. 1A) and identify trauma susceptibility/resilience. A pre-trauma ASR session (day −1) was carried out to measure ASR baseline the day before the traumatic procedure (24 h restraint stress, day 0, Chu et al., 2016). This was done to assemble two groups of mice [controls (C) and trauma-exposed (TE)] with similar average ASR baseline. C and TE mice were given two other ASR sessions, 14 (ASR 1, day 15) and 28 days (ASR 2, day 29) post-trauma respectively. Some mice were further tested two months post-trauma (day 56) in a third ASR session (ASR 3). The post-trauma change of ASR was analyzed both in terms of magnitude and latency and expressed as percentage of ASR baseline because of the high variability among animals (Longenecker et al., 2018). The change of startle magnitude was calculated by using the following formula: [(post-trauma magnitude – baseline magnitude) ×100/baseline magnitude]. The change of startle latency, whose decrease is a sign of hypervigilance (Lebow et al., 2012), was calculated by using the following formula: [(post-trauma latency – baseline latency) x 100/baseline latency].

To identify susceptibility and resilience of TE mice to the trauma, we developed a novel individual screening by using a simple mathematical tool, namely the z-normalization. This tool is widely used in clinical studies and also successfully employed in rodent studies (Guilloux et al., 2011) to measure emotionality dimensions that normally can diverge across time such as ASR (Longenecker et al., 2018). The z-scores originating from z-normalization reveal how many standard deviations an observation (X) is above or below the mean [(μ), with its standard deviation (σ)] of a control group: $Z = (X-μ)/σ$.

Here, the long-term changes of ASR of mice were z-normalized to obtain an individual score that we defined "arousal score".

AROUSAL score = [(X-μ/σ *startle magnitude,* day 15, 29 + X-μ/σ *startle latency,* day 15, 29)/4].

Taking into consideration that the vast majority of C mice showed an arousal score below 1, we empirically segregated TE mice by choosing a susceptibility threshold of 1. TE mice that showed an arousal score ≥1 were classified as susceptible, while TE mice with an arousal score <1 were classified as resilient.

2.2.2. Experiment 2: assessment of fear reactivity to and avoidance of a trauma-related cue

Intrusion symptoms such as marked physiological reactions to internal or external trauma-related stimuli [criterion B, DSM-5; (American Psychiatric Association DSM-5 Task Force, 2013)] and avoidance of trauma-related stimuli (criterion C, DSM-5; (American Psychiatric Association DSM-5 Task Force, 2013)] represent hallmark symptoms of PTSD. To model these symptoms, we evaluated fear reactivity to and avoidance of a trauma-related cue of susceptible and resilient mice, which were exposed to a neutral odor [lemon oil, the conditioned

stimulus (CS) or trauma-related cue] during the trauma [24 h restraint stress, the unconditioned stimulus (US)], in an odor-cued fear conditioning paradigm (Fig. 1G).

2.2.3. Experiment 3: assessment of avoidance-like behavior, social/cognitive function and depressive-like behavior

The general avoidance of situations that are not linked to the trauma (Sheynin et al., 2017) can be successfully modelled in rodents using approach-avoidance conflict paradigms. Here, the avoidance-like behavior of control, susceptible and resilient mice was assessed both in the OF (day 31) and EPM (day 32) tests (Fig. 2A).

Social isolation and cognitive deficits [criterion D, DSM-5; (American Psychiatric Association DSM-5 Task Force, 2013)] characterize PTSD and contribute to the impairment in social, occupational, or other important areas of functioning (criterion G, DSM-5; (American Psychiatric Association DSM-5 Task Force, 2013; Morena et al., 2017)]. In particular, patients with PTSD may experience social cognition deficits, namely disrupted processing (perception, attention or memory) of social information (Stevens and Jovanovic, 2019). In an attempt to model also this clinical aspect, here the same control, susceptible and resilient mice
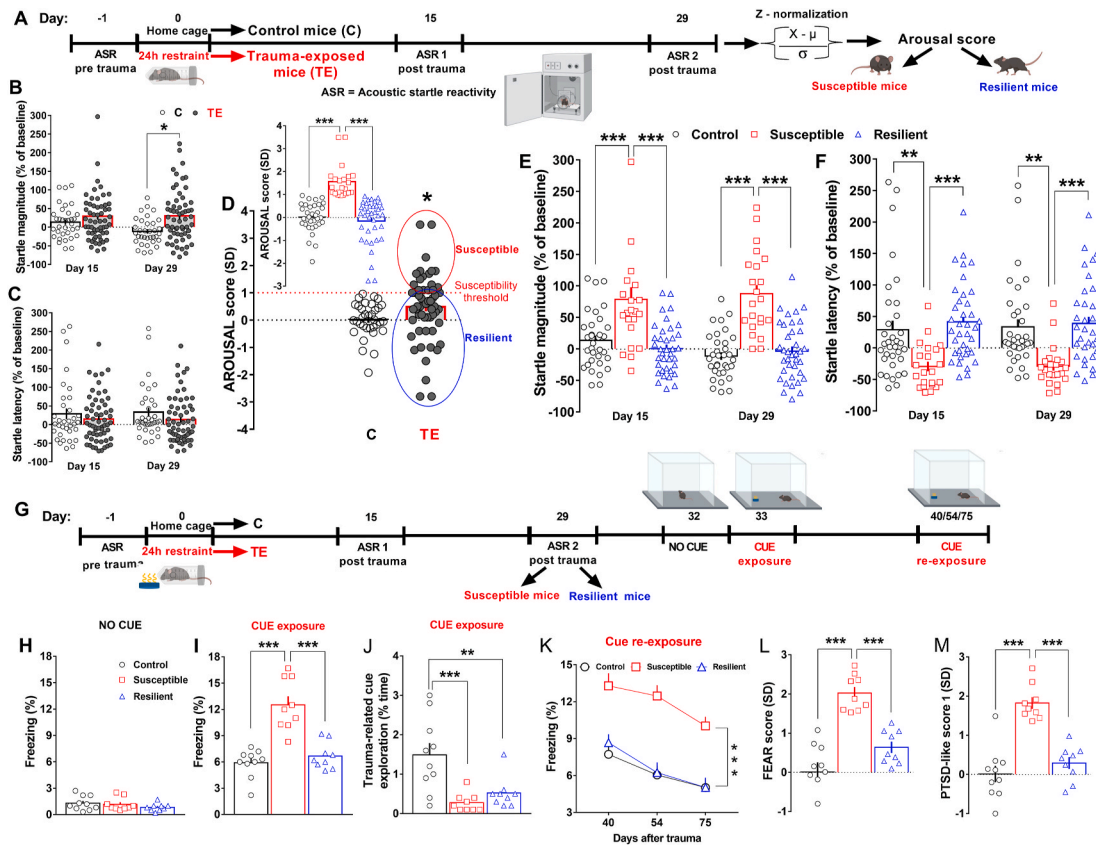

Fig. 1. *Susceptible mice exhibited long-lasting hyperarousal and exaggerated fear responses to trauma-related cue, while resilient mice adopted active coping strategies showing normal behavior.* **(A)** Experimental procedure conceived to shape the AIS model, which identified susceptible and resilient subpopulations. **(B)** Startle magnitude (% of baseline, *Stress,* $F_{(1, 91)} = 6.244$, $P = 0.0143$) and **(C)** startle latency (% of baseline) of control mice (C, n = 34) and trauma-exposed mice (TE, n = 59) tested in the ASR 1 and ASR 2 post-trauma sessions. **(D)** AROUSAL score of C and TE mice. The red dotted line, indicating 1 standard deviation as susceptibility threshold, divides susceptible (red circle) from resilient (blue circle) mice (C vs TE: P < 0.05); Inset: AROUSAL score after segregation in susceptible (n = 22) and resilient (n = 37) mice (*Stress susceptibility,* $F_{(2, 90)} = 35.66$, $P < 0.0001$). **(E)** Startle magnitude (% of baseline, *Stress susceptibility,* $F_{(2, 90)} = 32.65$, $P < 0.0001$) and **(F)** startle latency (% of baseline, *Stress susceptibility,* $F_{(2, 90)} = 11.35$, $P < 0.0001$) of control mice, susceptible mice and resilient mice identified through the AIS model. **(G)** Experimental procedure conceived for the longitudinal assessment of control (n = 10), susceptible (n = 9) and resilient mice (n = 9) from a different cohort, which were exposed to a neutral odor [lemon oil, the CS or trauma-related cue] during the restraint procedure (US), and were then assessed in an odor-cued fear conditioning test post-trauma. **(H)** Freezing behavior (% time) expressed during the no cue exposure session. **(I)** Freezing behavior (% time) expressed during the cue exposure session (*Stress susceptibility,* $F_{(2, 25)} = 27.09$, $P < 0.0001$). **(J)** Exploration (% time) of the trauma-related cue during the cue exposure session (*Stress susceptibility,* $F_{(2, 25)} = 10.27$, $P < 0.0001$). **(K)** Freezing behavior (% time) expressed during the cue re-exposure sessions (*Stress susceptibility,* $F_{(2, 25)} = 21.27$, $P < 0.0001$; *Time,* $F_{(2, 50)} = 25.69$, $P < 0.0001$). **(L)** FEAR score (*Stress susceptibility,* $F_{(2, 25)} = 28.8$, $P < 0.0001$). **(M)** PTSD-like score 1 (*Stress susceptibility,* $F_{(2, 25)} = 30.62$, $P < 0.0001$). Unpaired *t*-test, two-way repeated measures (RM) ANOVA or one-way ANOVA followed by Bonferroni *post hoc* test: *P < 0.05, **P < 0.01, ***P < 0.001. Values are expressed as means ± s. em. (For interpretation of the references to color in this figure legend, the reader is referred to the Web version of this article.)

previously assessed for their avoidance-like behavior, were further tested in the 5-trial SM test (day 34–35) that evaluates social memory, namely the capacity to recognize novel versus familiar mice (Fig. 2A).

Many individuals with PTSD may also receive a diagnosis of major depressive disorder (Flory and Yehuda, 2015). For this reason, other control, susceptible and resilient mice were assessed in the FST [day 43 in line with (Chu et al., 2016); Fig. 3A], which provides measure of depressive-like behavior.

2.2.4. Experiment 4: assessment of PTSD candidate genes mRNA expression in brain regions of interest in PTSD

Human findings indicate that PTSD is associated with altered gene expression (Smoller, 2016). To validate the segregation in susceptible and resilient mice obtained by the AIS model, we investigated the expression of four of the most promising and studied PTSD candidate genes, namely FK506 binding protein 5 (FKBP5), Serum/glucocorticoid-regulated kinase 1 (SGK1), the gene encoding for glucocorticoid receptor (NR3C1), and brain derived neurotropic factor (BDNF), which are important modulators of the stress system and have been found altered in individuals with PTSD (Binder et al., 2008; Breen et al., 2019; Girgenti and Duman, 2018; Lian et al., 2014; Yehuda et al., 2009; Zhang et al., 2014). The expression of these genes was evaluated in a triad of brain regions, medial prefrontal cortex (mPFC), amygdala (Amy), hippocampus (HIP), which according to neuroimaging studies

are involved in triggering PTSD symptoms (Garfinkel et al., 2014; Karl et al., 2006; Lisieski et al., 2018; Tovote et al., 2015), as well as in the hypothalamus (HT) that coordinates HPA axis responses to stress (Smith and Vale, 2006). The day after behavioral procedures (day 36, Fig. 4A) mice were sacrificed in order to dissect brain regions.

2.2.5. Experiment 5: assessment of PTSD candidate genes mRNA expression in the whole blood and HPA axis dysfunction

To further validate the segregation in susceptible and resilient mice obtained by the AIS model, possible variations in the expression of FKBP5 and SGK1, which have been found altered in blood of individuals with PTSD (Breen et al., 2019; Yehuda et al., 2009), were assessed in the blood of control, susceptible and resilient mice that were sacrificed the day after the segregation (day 30, Fig 5A).

As individuals with PTSD show long-term dysfunction of the HPA axis (Mehta and Binder, 2012), we further measured pre-trauma basal serum corticosterone level as well as post-trauma long-term basal serum corticosterone level in other control, susceptible and resilient mice (Fig 5A).

2.2.6. Experiment 6: assessment of synaptic transmission and plasticity in the hippocampal CA1 region

PTSD has been associated with altered neuroplasticity, especially in the HIP (Abdallah et al., 2017), in line with evidences demonstrating
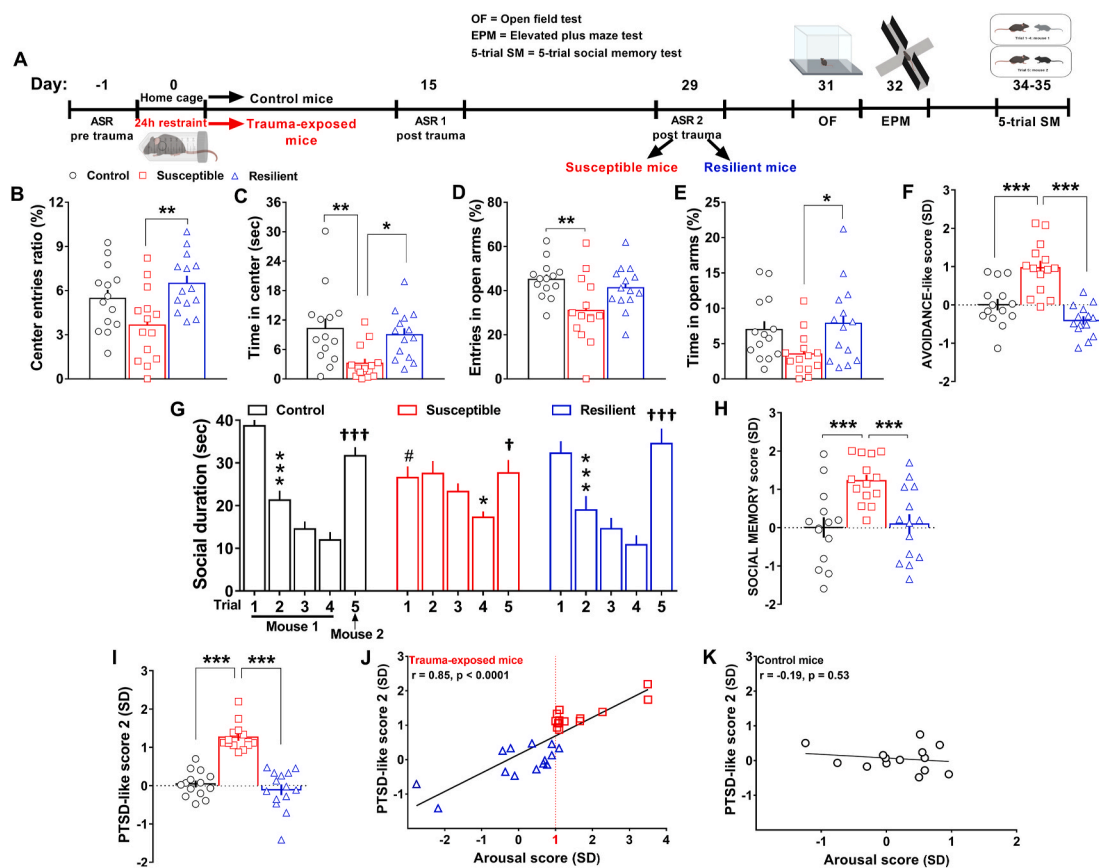

Fig. 2. Susceptible mice identified by the AIS model displayed increased avoidance-like behavior and social memory impairment, while resilient mice behaved similar to control mice. **(A)** Experimental procedure conceived for the assessment of control (n = 14), susceptible (n = 14) and resilient mice (n = 14) in the OF test, EPM test and 5-trial SM test. **(B)** Center entries ratio (*Stress susceptibility*, $F_{(2, 39)} = 5.957$, P = 0.0055) and **(C)** time spent in center of the OF (*Stress susceptibility*, $F_{(2, 39)} = 6.237$, P = 0.0045). **(D)** Entries in open arms (*Stress susceptibility*, $F_{(2, 39)} = 5.526$, P = 0.0077) and **(E)** time in open arms of EPM (*Stress susceptibility*, $F_{(2, 39)} = 3.629$, P = 0.036). **(F)** AVOIDANCE-like score (*Stress susceptibility*, $F_{(2, 39)} = 22.24$, P < 0.0001). **(G)** Social duration during the 5-trial SM test [*Trial*, $F_{(4, 156)} = 52.49$, P < 0.0001, *Stress susceptibility* x *trial*, $F_{(8, 156)} = 6.144$, P < 0.0001; Bonferroni post hoc test: *p < 0.05,***p < 0.001 vs each specific trial 1 (habituation); #P < 0.05 vs the trial 1 of control mice,†p < 0.05, †††p < 0.001 vs each specific trial 5 (dishabituation)]. **(H)** SOCIAL MEMORY score (*Stress susceptibility*, $F_{(2, 39)} = 8.604$, P < 0.0001). **(I)** PTSD-like score 2 (*Stress susceptibility*, $F_{(2, 39)} = 47.31$, P < 0.0001). **(J)** Linear correlation between the arousal score and the PTSD-like score 2 of trauma-exposed mice (r = 0.85, p < 0.0001) and **(K)** control mice. Two-way RM ANOVA or one-way ANOVA followed by Bonferroni *post hoc* test *P < 0.05, **P < 0.01, ***P < 0.001. Values are expressed as means ± s. e. m.

that stress alters synaptic function in the hippocampal glutamatergic synapse (Pavlovsky et al., 2012). Thus, to further validate the AIS model, we investigated whether trauma susceptibility/resilience obtained by the AIS model was linked to changes in synaptic transmission and plasticity in the HIP. Because human data show hippocampal CA1 abnormalities (Chen et al., 2018) in individuals with PTSD and the CA1 subfield has the major influence on fear memory among the hippocampal subfields (Furini et al., 2014), extracellular electrophysiological recordings were carried out at CA3-CA1 synapses of slices from hippocampi obtained from control, susceptible and resilient mice (Fig. 6A).

2.2.7. 7. Experiment 7: effect of chronic treatment with paroxetine

To assess the predictive validity of our model, control, susceptible and resilient mice were chronically treated with a clinically relevant dose (10 mg/kg, i. p.) of paroxetine (first-line pharmacotherapy for PTSD) that was shown to be effective in improving PTSD-like behaviors (Philbert et al., 2013, 2015), from the day after the segregation (day 30) to the end of behavioral experiments (day 48) as illustrated in the timeline (Fig. 7A). In particular, mice underwent post-segregation ASR sessions on the day 36 and 43 (ASR 3 and ASR 4), the OF on the day 44, the EPM on the day 45 and the 5-trial SM on the days 47/48. To evaluate whether or not paroxetine modified PTSD candidates gene expression, brain regions were dissected the day after behavioral procedures (day 49).

2.3. The AIS model (traumatic procedure)

C57BL6/J mice are more resilient to stress compared to other strains (Jacobson and Cryan, 2007; Mozhui et al., 2010; Savignac et al., 2011) and have been specifically reported resilient to acute restraint stress of short duration (Flint and Tinkle, 2001). To trigger long-term trauma susceptibility and avoid the possible occurrence of only long-term trauma resilience, we chose a restraint traumatic procedure of long duration (24 h), which also provides the advantage of being a traumatic procedure very easy to carry out compared to other commonly used traumatic procedures. Mice were gently put in Falcon 50 mL conical centrifuge cubes and exposed to 24 h of restraint from 3:00 pm (3 h before the beginning of the dark phase) to 3:00 pm of the next day.

2.4. Acoustic startle reactivity (ASR) sessions

Mice were tested during the light phase from 9.00 a.m. to 3.00 p.m. in illuminated, ventilated and sound-attenuated startle chambers (SR-Lab System, San Diego Instruments, San Diego, CA, United States) containing a Plexiglas cylinder equipped with a piezoelectric accelerometer to detect animal movement. Each chamber was calibrated according to manufacturer's guidelines before the start of each experiment. Mice were placed in the cylinders of the chambers for a 5-min acclimation period with a 65 dB(A) background noise, and then exposed to 10 acoustic startle stimuli [40 ms — 100 dB(A) noise bursts], which were delivered with variable inter trial intervals of 21, 7, 20, 9, 14, 21, 11, 8, and 23 s to avoid habituation and compensatory mechanisms (Olson et al., 2011). Both magnitude (V max, peak of the response) and latency (T max, time at which the V max occurs) were considered for measurement of the ASR.

2.5. Behavioral paradigms

Behavior of mice was recorded (Sony Videocam PJ330E) and subsequently analyzed by two experts, well-trained researchers. All the apparatuses were cleaned with a 70% ethanol solution in between each test to prevent olfactory cues. All behavioral experiments were performed during the light phase from 9.00 a.m. to 3.00 p.m.

2.5.1. Odor-cued fear conditioning test

Mice were tested in an evenly illuminated (60 ± 1 lux) square open field (40 × 40 × 40 cm, Ugo Basile, Gemonio, Italy) after the segregation in susceptible and resilient subpopulations. The behavioral procedure consisted of a no cue exposure session, a cue exposure session and three cue re-exposure sessions, which were carried out at different time. Fear reactivity to the trauma-related cue was detected through the measurement of freezing behavior (% time), which was defined as the complete lack of movement except for that necessary for breathing. Avoidance of the trauma-related cue was identified by assessing explorative behavior of the trauma-related cue, which was defined as the mouse directing its nose toward the cap at a distance of < 2 cm.

2.5.2. Open field (OF) test

To assess avoidance-like behavior and locomotor activity, mice were tested in a square open field (40 × 40 × 40 cm, Ugo Basile, Gemonio, Italy) over a 5 min-period as previously reported (Torrisi et al., 2017). Avoidance-like behavior was measured by counting numbers of entries and time spent in the center of the open field.

2.5.3. Elevated plus maze (EPM) test

To further measure avoidance-like behavior, mice were tested in the EPM test as previously described with minor modifications (Leggio et al., 2015). Number of entries (%) and time spent (%) in the open arms of the EPM were used as parameters.

2.5.4. 5-Trial social memory (5-trial SM) test

To evaluate the social/cognitive domain, mice were tested as previously reported (Leggio et al., 2019b) with minor changes. If the social memory is intact, mice normally decrease their social interaction with a stimulus mouse (mouse 1) over the course of multiple exposures (trial 1–4, habituation), and then increase their social interaction with a different stimulus mouse (mouse 2) (trial 5, dishabituation) in the last trial of the test.

2.5.5. Forced swim test (FST)

To measure depressive-like behavior, immobility time as well as latency until the first episode of immobility of mice were assessed in the FST as previously reported (Gerhard et al., 2020).

2.6. Behavioral z-scoring: Fear score, avoidance like-score, social memory score and PTSD-like scores.

Because PTSD is characterized by different complementary symptoms over time, we also applied z-normalization to all behavioral tests that mice further underwent, to create specific scores for each mouse (fear score, avoidance like-score, social memory score and PTSD-like score). Indeed, the z-normalization not only allows data integration deriving from different and complementary parameters of a specific behavioral paradigm in a single score, but it can also be used to obtain an overall score arising from the z-normalization of all the behavioral parameters observed in the same mouse exposed to a battery of different tests. Moreover, it decreases the behavioral noise related to the use of multiple tests, which enhances the reliability of behavioral phenotyping (Guilloux et al., 2011). The directionality of z-scores was adjusted such that maladaptive behavior is represented by positive standard deviations.

A "fear score" was calculated for the odor-cued fear conditioning test by z-normalizing the % of freezing during the exposure and the re-exposure sessions and the % of time exploring the trauma-related cue:

FEAR score = [(X-μ/σ freezing, day 32 + X-μ/σ exploration time of trauma-related cue, day 32 + X-μ/σ freezing, day 40, 54, 75)/5].

Similarly, an "avoidance-like score" as well as a "social memory score" were calculated by z-normalizing the parameters we analyzed in the OF, EPM and 5-trial SM:

AVOIDANCE-like score = [(X-μ/σ center entries ratio + X-μ/σ time in the center + X-μ/σ entries open arms + X-μ/σ time open arms)/4].
SOCIAL MEMORY score = [(X-μ/σ trial 1,2,3,4,5)/5].

Finally, the z- normalization was further utilized to create a PTSD-like score that represents a single value originating from all the previous scores. Different PTSD-like scores were calculated according to the battery of tests each individual animal underwent.

PTSD-like score 1 = [(AROUSAL score + FEAR score)/2].
PTSD-like score 2 = [(AROUSAL score + AVOIDANCE-like score + SOCIAL MEMORY score)/3].

For the pharmacological experiments, the arousal score included in the PTSD-like score 2 was calculated considering the ASR sessions post trauma (ASR 3 and 4).

2.6. Pharmacological treatment

Mice were chronically treated with paroxetine hydrochloride (Cayman Chemical, Ann Arbor, Michigan 48108 USA) or vehicle. Paroxetine was dissolved firstly in dimethyl sulfoxide (DMSO) and then diluted with distilled water to obtain a final solution containing 3% of DMSO. Paroxetine and vehicle (3% solution distilled water/DMSO) were administered i. p. by using an injection volume of 10 ml/kg. On the day of the tests, paroxetine and vehicle were administered 2 h before the beginning of the test.

2.7. Analysis of gene expression by real-time quantitative RT-PCR

For analysis of gene expression in brain areas, mice were killed via cervical dislocation 24 h after the 5-trial SM, during the light phase from 10.00 a.m. to 2.00 p.m. HIP, mPFC, HT and Amy were microdissected according to established protocols (Leggio et al., 2019a; Zapala et al., 2005). One cohort of mice was used to microdissect the mPFC and HIP and another independent one was used to microdissect the HT and Amy. For analysis of gene expression in the whole blood, mice were killed via cervical dislocation and decapitated to collect trunk blood. Blood was directly collected in 4 μl-EDTA 0.5 M-containing Eppendorf and gently shaken to avoid coagulation. RT-PCR was performed as previously reported (Cosentino et al., 2019; Leggio et al., 2015).

2.8. Corticosterone measurement

A small amount of blood was collected from the same mice (C and TE) after bleeding of the submandibular vein as previously described (Golde et al., 2005), both 5 to 6 h before (9:00-10:00 a.m.) the start of the trauma and the day after (9:00-10:00 a.m.) the segregation in subpopulation. Blood was directly collected in a sterile Eppendorf and kept at room temperature for 3 h. Afterwards, it was centrifuged a $1000 \times g$ for 15 min to isolate serum. ELISA assay was performed using a Corticosterone ELISA kit (Cayman chemical, Michigan, U.S.A.) according to manufacturer's instructions and as previously reported (Cosentino et al., 2019). Each sample was run in triplicate.

2.9. Electrophysiological recordings

Mice were randomly selected and killed via cervical dislocation prior to the recording. These experiments were performed by an operator blind with respect to subpopulation. Extracellular electrophysiological field recordings were performed on 400 μm transverse hippocampal slices as previously described (Gulisano et al., 2019). We first measured basal synaptic transmission (BST) by stimulating with a series of increasing voltage pulses (from 5 to 35 V). In LTP experiments, baseline was recorded every minute for 15 min by a stimulus intensity evoking a response of 35% of the maximum evoked response in BST. LTP was induced by a theta-burst stimulation (trains of 10×100 Hz bursts with five pulses *per* burst with a 200 ms inter-burst interval at the test pulse intensity). After induction of LTP, every slice was recorded for 120 min. Triangular surface plots representing the individual slices in each condition were generated in Python 3 with Matplotlib 3.1.1 libraries.

2.10. Statistical analysis

Sample size was determined by using power analysis and was thus similar to that of studies using related methods (Lopez et al., 2017). Each experimental group consisted of a minimum of five mice. Data were analyzed using GraphPad Prism 7 (GraphPad Software, La Jolla, CA, USA). To assess data distribution, the D'Agostino-Pearson omnibus normality test was carried out. The Levene's test was also used to verify equality of variances. All data assumed a normal distribution and then they were subjected to parametric tests (one- or two-way ANOVA and two-way ANOVA with repeated measures when appropriate). For all data analyses, upon confirmation of significant main effects, differences among individual means were assessed using Bonferroni post-hoc test. P values of <0.05 were considered significant. Pearson's correlation analysis was performed to assess the linear correlation between the AROUSAL score and the PTSD-like score. Pearson's correlation analysis was further performed to assess the linear correlation between the AROUSAL score and mRNA expression of the PTSD-candidate genes. ANOVA with repeated measure was used to analyze BST curves and LTP for 120 min recording after tetanus. The estimate of dispersion is shown as the standard error of the mean (s.e.m.), and variances were found to be similar among groups. All data are presented as means ± s. e.m.

3. Results

3.1. Susceptible and resilient mice were identified through the AIS model

In line with the variable responses displayed by individuals exposed to the same traumatic event, we observed heterogeneity in the ASR of TE mice with a general significant increase of startle magnitude (Fig. 1B, *Stress,* $F_{(1, 91)} = 6.244, P = 0.0143$) and a not significant decrease of startle latency (Fig. 1C), detectable in both post-trauma ASR sessions that were carried out on the same mice 14 (ASR 1) and 28 days (ASR 2) post-trauma respectively. To more finely capture the manifestation of hyperarousal over time, we used the z-normalization that allows integrating several converging and complementary data. The z-normalization allowed us to segregate TE mice in susceptible and resilient groups by calculating the arousal score (Fig. 1D, *Stress susceptibility,* $F_{(2, 90)} = 35.66, P < 0.0001$). This approach was useful, as it uncovered a post-trauma hyperarousal only in susceptible mice. Indeed, susceptible mice (25%–35%, across experiments) showed a significant higher startle magnitude (Fig. 1E, *Stress susceptibility,* $F_{(2, 90)} = 32.65, P < 0.0001$) as well as a faster reaction time (decrease of startle latency; Fig. 1F, *Stress susceptibility,* $F_{(2, 90)} = 11.35, P < 0.0001$) to the startle stimuli compared to control mice during both ASR1 and ASR2. In contrast, resilient mice (65%–75%, across experiments) showed arousal level similar to control mice both in terms of startle magnitude (Fig. 1E) and latency (Fig. 1F) during both ASR1 and ASR2. Interestingly, the hyperarousal showed by susceptible mice was persistent, given that it was still present two months post-trauma (Fig. S1A startle magnitude, *Stress susceptibility,* $F_{(2, 17)} = 4.03, P = 0.037$. Fig. S1B startle latency, *Stress susceptibility,* $F_{(2, 17)} = 6.53, P = 0.0079$. Fig. S1C arousal score, *Stress susceptibility,* $F_{(2, 17)} = 9.543, P = 0.0017$). Besides, we observed a persistent hyperarousal only in susceptible mice, which became significantly more pronounced over time (only in terms of startle magnitude) by adding a further stressor (chronic I.P. treatment; Fig. S1D startle magnitude, *Stress susceptibility,* $F_{(2, 19)} = 13.46, P = 0.0002$; *Treatment* $F_{(3, 57)} = 2.81, P = 0.048$. Fig. S1E startle latency, *Stress susceptibility,* $F_{(2, 19)} = 6.76, P = 0.0060$). Also, a retrospective analysis of our data revealed low pre-trauma startle reactivity only in susceptible mice. They exhibited in fact, significant lower pre-trauma startle magnitude (Fig. S1F, *Stress susceptibility,* $F_{(2, 197)} = 4.863, P = 0.0087$) and higher pre-trauma startle latency compared to both control and resilient mice (Fig. S1G, *Stress susceptibility,* $F_{(2, 197)} = 17.52, P < 0.0001$).

3.2. Susceptible mice exhibited long-lasting exaggerated fear responses to trauma-related cue

During the no cue exposure session (day 32), there was no difference in basal freezing time among groups (Fig. 1H). Importantly, only susceptible mice exhibited exaggerated fear responses to trauma-related cue during the cue exposure session (day 33), as indicated by the significant longer freezing time in comparison with control mice (Fig. 1I, *Stress susceptibility*, $F_{(2, 25)} = 27.09, P < 0.0001$). By contrast, resilient mice behaved similarly to control mice (Fig. 1I). Both susceptible and resilient mice avoided to explore the trauma-related cue as displayed by the significant lower cue exploration time compared to the control mice (Fig. 1J, *Stress susceptibility*, $F_{(2, 25)} = 10.27, P < 0.0001$). This latter observation indicates that also resilient mice learned to associate the cue with the trauma and thus they exhibited normal fear memory encoding/recall without showing abnormal fear responses. More importantly, the exaggerated fear responses displayed by susceptible mice were persistent, in fact they were further observed during cue re-exposure sessions (day 40, 54, 75), the last of which was performed two months and a half after the trauma (Fig. 1K, *Stress susceptibility*, $F_{(2, 25)} = 21.27, P < 0.0001$; *Time*, $F_{(2, 50)} = 25.69, P < 0.0001$). Overall, fear score (Fig. 1L, *Stress susceptibility*, $F_{(2, 25)} = 28.8, P < 0.0001$) and PTSD-like score 1 (Fig. 1M, *Stress susceptibility*, $F_{(2, 25)} = 30.62, P < 0.0001$) of susceptible mice were significantly higher in comparison with scores of both control and resilient mice.

3.3. Susceptible mice showed increased avoidance-like behavior and social/cognitive dysfunction, but they did not show depressive-like phenotypes

Susceptible mice exhibited a significant increase of avoidance-like behavior. In the OF test, they indeed significantly decreased the number of entries in the center compared to resilient mice (Fig. 2B, *Stress susceptibility*, $F_{(2, 39)} = 5.957, P = 0.0055$) and they significantly decreased the time spent in the center compared to both control and resilient mice (Fig. 2C, *Stress susceptibility*, $F_{(2, 39)} = 6.237, P = 0.0045$). Moreover, in the EPM test, susceptible mice significantly decreased the number of entries in the open arms (Fig. 2D, *Stress susceptibility*, $F_{(2, 39)} = 5.526, P = 0.0077$) compared to control mice and they significantly decreased the time spent in the open arms compared to resilient mice (Fig. 2E, *Stress susceptibility*, $F_{(2, 39)} = 3.629, P = 0.036$). Conversely, resilient mice adopted active coping strategies behaving as control mice (Fig. 2B–E). Of note, there was no basal difference in body weight among control, susceptible and resilient mice, and all groups significantly increased their body weight one month post-trauma (Fig. S2A, *Time*, $F_{(1, 39)} = 219, P < 0.0001$). In addition susceptible mice showed a normal locomotion (total crossings) in the OF (Fig S2B), but a slight significant decrease of locomotion (total entries) in the EPM (Fig. S2C, *Stress susceptibility* $F_{(2, 39)} = 3.888, P = 0.029$). As a whole, susceptible mice showed a significant higher avoidance-like score in comparison with both control and resilient mice (Fig. 2F, *Stress susceptibility*, $F_{(2, 39)} = 22.24, P < 0.0001$).

Both control and resilient mice exhibited an intact social memory. They, indeed, progressively lost interest in the social investigation of a stimulus male mouse (mouse 1) over the course of the trials 1–4 (habituation) and then they were interested in the social investigation of a novel stimulus male mouse (mouse 2; dishabituation; Fig. 2G). Interestingly, susceptible mice showed a marked social memory impairment, as indicated by the delayed habituation to the mouse 1 that occurred in the last (fourth) trial, as well as a significant decrease of social investigation in the first trial compared to control mice (Fig. 2G, *Trial*, $F_{(4, 156)} = 52.49, P < 0.0001$, *Stress susceptibility* x *Trial*, $F_{(8, 156)} = 6.144, P < 0.0001$). Overall, susceptible mice displayed significant higher social memory score (Fig. 2H, *Stress susceptibility* $F_{(2, 39)} = 8.604, P < 0.0001$) and PTSD-like score 2 (Fig. 2I, *Stress susceptibility*, $F_{(2, 39)} = 47.31, P < 0.0001$) compared to both control and resilient mice. Interestingly, the

development of a high arousal score predicted the development of a high PTSD-like score 2, as shown by a significant positive correlation between the arousal score and the PTSD-like score 2 of TE mice (Fig. 2J, $r = 0.85, p < 0.0001$). Conversely, there was no significant linear correlation between these two scores in C mice (Fig. 2K).

Neither susceptible nor resilient mice displayed long-term depressive-like behavior. Indeed, there were no significant differences between the three groups both in the latency to immobility time (Fig. 3B) and total immobility time (Fig. 3C).

3.4. Novel and divergent transcriptional signatures driven by PTSD candidate genes as well as peripheral marks of HPA dysfunction corroborated the segregation in subpopulations and correlated with trauma susceptibility/resilience

Susceptible and resilient mice showed divergent expression of PTSD candidate genes according to PTSD-related brain regions. FKBP5 was significantly up-regulated in the mPFC of susceptible mice, whereas it was significantly down-regulated in the Amy, HIP and HT of resilient mice (Fig. 4B, *Stress susceptibility*: mPFC, $F_{(2, 22)} = 5.055, P = 0.0156$; HIP, $F_{(2, 22)} = 4.931, P = 0.017$; Amy, $F_{(2, 13)} = 5.132, P = 0.022$; HT, $F_{(2, 13)} = 5.235, P = 0.0215$). There was also a positive significant correlation between the arousal score and the expression of FKBP5 exclusively in the HIP (Fig. 4C, $r = 0.52, P = 0.04$). Regarding SGK1, it was significantly up-regulated only in the HT of susceptible mice and unchanged in the other brain regions (Fig. 4D, *Stress susceptibility*: $F_{(2, 13)} = 4.318, P = 0.0303$). No correlation between the arousal score and the expression of SGK1 was detected in any brain regions (Fig. 4E). Intriguingly, BDNF gene expression was found significantly up-regulated in the mPFC and HC (vs resilient) of susceptible mice and in the HT of resilient mice, but at the same time, it was down-regulated in the Amy of resilient mice (Fig. 4F, *Stress susceptibility*: mPFC, $F_{(2, 22)} = 4.65, P = 0.0206$; HIP, $F_{(2, 22)} = 3.50, P = 0.047$; Amy, $F_{(2, 13)} = 27.79, P < 0.0001$; HT, $F_{(2, 13)} = 10.7, P = 0.0018$). Moreover, there were positive significant correlations between the arousal score and BDNF expression in the HIP and Amy (Fig. 4G, HIP, $r = 0.77, P = 0.0006$; Amy, $r = 0.67, P = 0.03$). The expression of NR3C1 further changed depending on brain regions and subpopulations. It was found significantly up-regulated in the HT of susceptible mice and down-regulated in the mPFC and Amy of resilient mice respectively (Fig. 4H, *Stress susceptibility*: mPFC, $F_{(2, 22)} = 7.429, P = 0.0034$; Amy, $F_{(2, 13)} = 7.958, P = 0.0055$; HT, $F_{(2, 13)} = 6.471, P = 0.0112$). Finally, there was a positive significant correlation between the arousal score and the expression of NR3C1 in the mPFC (Fig. 4I, $r = 0.78, P = 0.0006$).

With regard to the PTSD candidate genes mRNA expression in the whole blood, a significant down-regulation of both FKBP5 (Fig. 5B, *Stress susceptibility*, $F_{(2, 12)} = 10.82, P = 0.0021$) and SGK1 (Fig. 5D, *Stress susceptibility*, $F_{(2, 12)} = 3.945, P = 0.048$) was detected in susceptible but not resilient mice. Furthermore, a significant negative correlation between the arousal score and the expression of FKBP5 (Fig. 5C, $r = -0.79, P = 0.0066$) but not SGK1 (Fig. 5E) in the whole blood of mice was revealed.

Regarding the HPA axis function, there were no differences in pre-trauma basal corticosterone level between subpopulations. Interestingly, it was detected a significant higher post-trauma basal corticosterone level exclusively in susceptible mice compared to both their pre-trauma basal corticosterone level, and compared to the post-trauma basal corticosterone level of control and resilient mice, (Fig. 5F, *Stress susceptibility*, $F_{(2, 21)} = 4.984, P = 0.0169$; *Time* $F_{(1, 21)} = 7.306, P = 0.0133$; *Stress susceptibility* x *Time* $F_{(2, 21)} = 5.474, P = 0.0122$). Also, a significant positive correlation between the arousal score and the post-trauma corticosterone level was detected (Fig. 5G, $r = 0.75, P = 0.0006$).
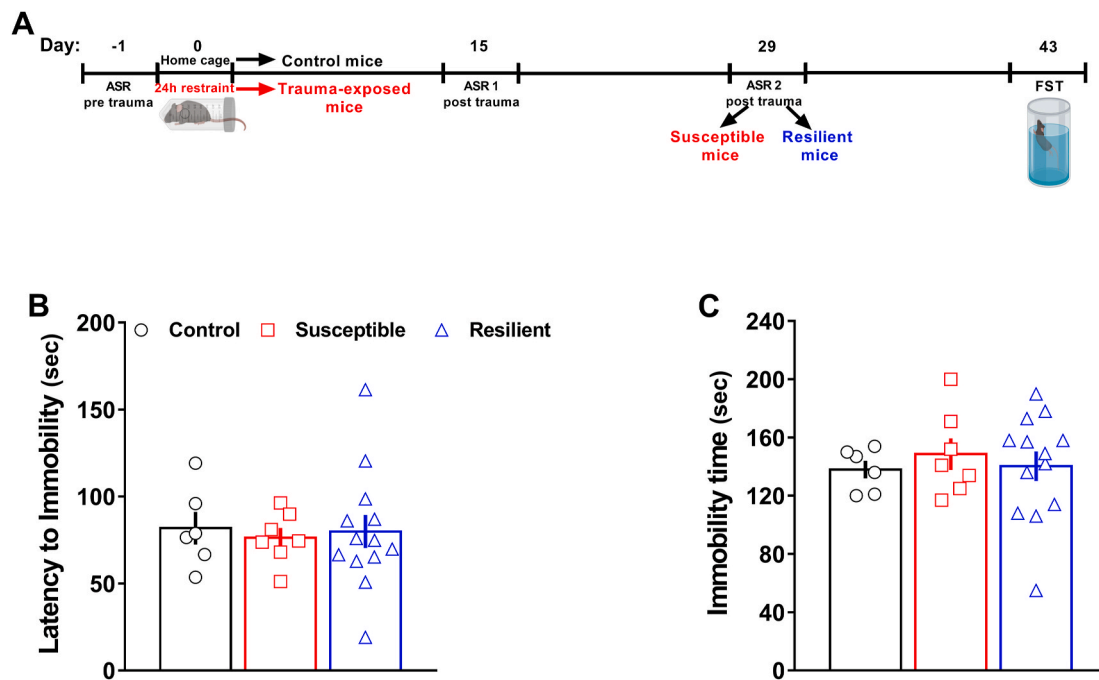
Fig. 3. *Both susceptible and resilient mice did not exhibit depressive-like phenotypes.* **(A)** Experimental timeline designed for the long-term assessment of control (n = 6), susceptible (n = 6) and resilient (n = 14) mice tested in the FST. **(B)** Latency to immobility and **(C)** total immobility time. One-way ANOVA followed by Bonferroni *post hoc* test. Values are expressed as means ± s. e. m.

3.5. Susceptible but not resilient mice exhibited impaired hippocampal synaptic plasticity

Basal synaptic transmission (BST) was not different among control, susceptible and resilient mice, either when analyzing fEPSP slope or fiber volley (FV) (Fig. 6B). Long-term potentiation (LTP), a type of synaptic plasticity thought to underlie memory formation, was significantly impaired in susceptible but not in resilient mice (Fig. 6C–D, *Stress susceptibility*, $F_{(1,13)} = 16.505$, P = 0.001), as also visible from triangular surface plots representing potentiation of individual slices for each experimental group (Fig. 6E–G).

3.6. Chronic treatment with paroxetine resulted effective in susceptible mice but detrimental in control and resilient mice

Paroxetine-treated susceptible mice exhibited a trend of higher startle magnitude (Fig. 7B, *ASR3: Treatment,* $F_{(1, 37)} = 6.024$, P = 0.019; *Stress susceptibility,* $F_{(2, 37)} = 18.88$, P < 0.0001. *ASR4: Treatment,* $F_{(1, 37)} = 3.84$, P = 0.049; *Stress susceptibility,* $F_{(2, 37)} = 14.25$, P < 0.0001) and lower startle latency (Fig. 7C, *ASR3: Treatment,* $F_{(1, 37)} = 12.02$, P = 0.0014; *Stress susceptibility,* $F_{(2, 37)} = 6.64$, P = 0.0034. *ASR4: Stress susceptibility,* $F_{(2, 37)} = 5.271$, P = 0.0097) compared to vehicle-treated susceptible mice, which significantly maintained their hyperarousal over time compared to control mice during both the ASR3 and ASR4. In addition, whereas paroxetine-treated control mice exhibited a trend of higher startle magnitude and a significant lower startle latency compared to vehicle-treated control mice during both the ASR3 and ASR4, paroxetine-treated resilient mice showed only a significant lower startle latency during the ASR4 compared to vehicle-treated resilient mice (Fig. 7B–C). As summarized through the calculation of the arousal score, paroxetine tended to worsen the hyperarousal of susceptible mice, induced a significant hyperarousal in control mice and marginally affect the arousal of resilient mice (Fig. 7D, *Treatment,* $F_{(1, 37)} = 8.67$, P = 0.0056; *Stress susceptibility,* $F_{(2, 37)} = 22.23$, P < 0.0001). Paroxetine-treated susceptible mice, subsequently tested in the OF and EPM tests, interestingly displayed a significant decrease of avoidance-like behavior compared to vehicle-treated susceptible mice, as indicated by the

significant augmented number of entries (Fig. 7E, *Treatment x Stress susceptibility* $F_{(2, 37)} = 10.45$, P = 0.0003) and time spent (Fig. 7F, *Treatment x Stress susceptibility* $F_{(2, 37)} = 7.45$, P = 0.0019) in the center of the OF, and by the significant augmented number of entries (Fig. 7G, *Treatment* $F_{(1, 37)} = 25.14$, P < 0.0001; *Treatment x Stress susceptibility* $F_{(2, 37)} = 22.68$, P < 0.0001) and time spent (Fig. 7H, *Treatment* $F_{(1, 37)} = 5.29$, P = 0.0272; *Treatment x Stress susceptibility* $F_{(2, 37)} = 8.77$, P = 0.0008) in open arms of EPM. Of Note, vehicle-treated susceptible mice further showed an increased avoidance-like behavior compared to vehicle-treated control mice (Fig. 7E–H). By contrast, paroxetine-treated resilient mice showed an almost significant decrease of number of entries and time spent in the center of the OF (Fig. 7E–F) and a significant decrease of number of entries and time spent in the open arms of the EPM compared to vehicle-treated resilient mice (Fig. 7G-H). In addition, paroxetine-treated control mice exhibited a significant decrease of number of entries and time spent both in the center of the OF (Fig. 7E–F) and open arms of the EPM (Fig. 7G-H). Overall, the avoidance-like score clearly showed the significant beneficial effect of paroxetine in susceptible mice as well as the detrimental effect in both control and resilient mice (Fig. 7I, *Treatment* $F_{(1, 37)} = 18.3$, P < 0.0001; *Treatment x Stress susceptibility* $F_{(2, 37)} = 30.48$, P < 0.0001). Of note, paroxetine did not affect the locomotion of control, susceptible and resilient mice in the OF test (Fig. S2D), but affected the locomotion of resilient mice in the EPM test (Fig. S2E, *Treatment,* $F_{(1, 37)} = 7.648$, P = 0.0088). Regarding the 5-trial SM test (day 47–48), paroxetine significantly ameliorated the impaired social memory of susceptible mice. In fact, paroxetine-treated susceptible mice did not exhibit social memory impairment, as indicated by a striking habituation to the mouse 1 during the first four trials and a dishabituation after the exposure to the mouse 2 on the fifth trial compared to vehicle-treated susceptible mice, which instead exhibited a marked social memory impairment (Fig. 7J, *Treatment* x *Trial,* $F_{(20, 144)} = 3.065$, P < 0.0001; *Trial,* $F_{(4, 144)} = 74.6$, P < 0.0001). No effects of paroxetine on social memory of both control mice and resilient mice were observed (Fig. 7J). Likewise the avoidance-like score, the social memory score visibly displayed the significant beneficial effect of paroxetine in susceptible mice (Fig. 7K, *Treatment x Stress susceptibility* $F_{(2, 37)} = 8.69$, P = 0.0008). Importantly, the further application of the z-
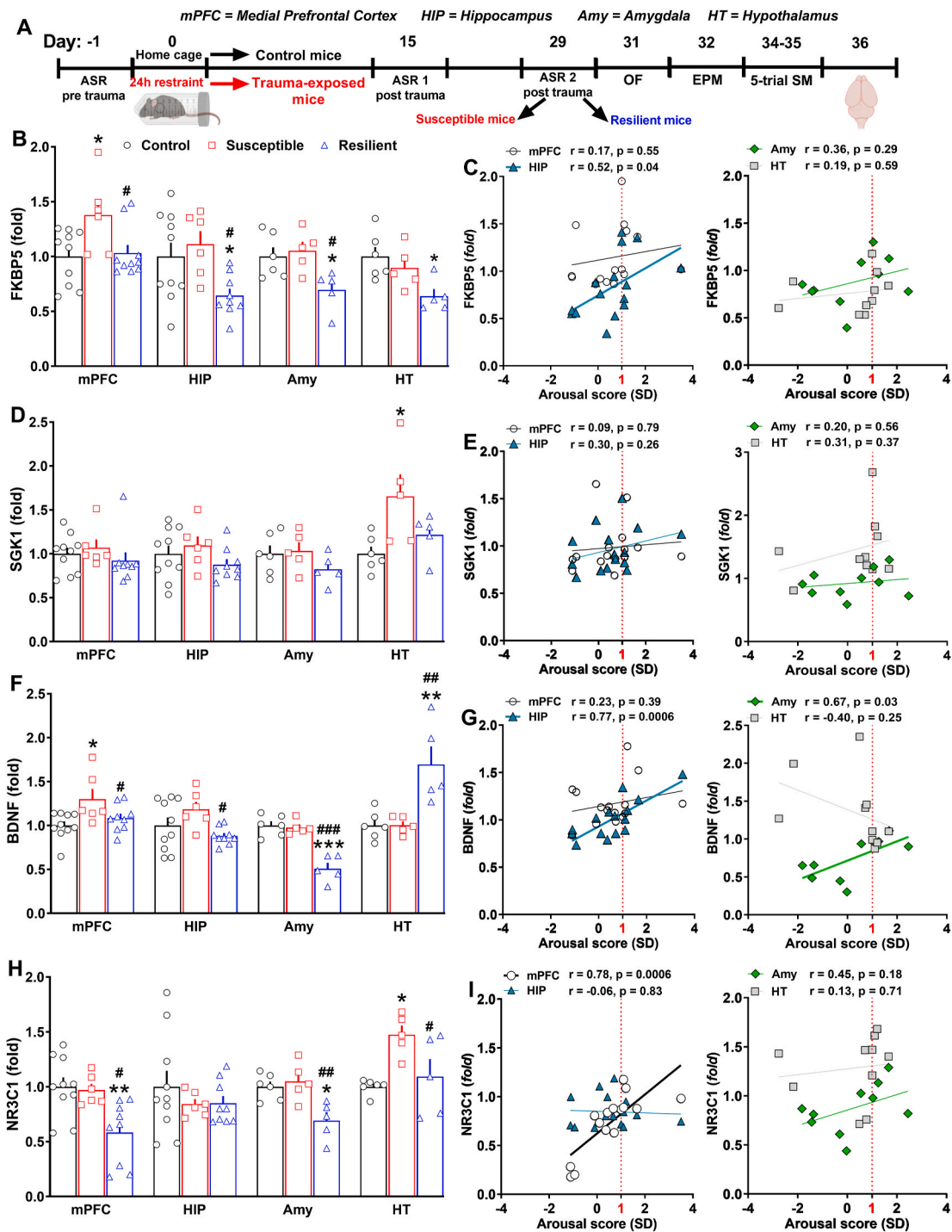
Fig. 4. *Divergent central transcriptional signatures driven by PTSD candidate genes corroborated the segregation in susceptible and resilient subpopulations revealed by the AIS model and correlated with trauma susceptibility/resilience.* **(A)** Timeline: the day after the end of the 5-trial SM test, control (n = 10), susceptible (n = 6) and resilient mice (n = 9) from one cohort were sacrificed to microdissect mPFC and hippocampus. Other control (n = 6), susceptible (n = 5) and resilient mice (n = 5) from an independent cohort were sacrificed to microdissect amygdala and hypothalamus. Abundance of transcripts was assessed by qPCR. **(B)** FKBP5 mRNA expression in the mPFC (*Stress susceptibility*, $F_{(2, 22)}$ = 5.055, P = 0.0156), HIP (*Stress susceptibility*, $F_{(2, 22)}$ = 4.931, P = 0.017), Amy (*Stress susceptibility*, $F_{(2, 13)}$ = 5.132, P = 0.022) and HT (*Stress susceptibility*, $F_{(2, 13)}$ = 5.235, P = 0.0215). **(C)** Linear correlation between the arousal score and the expression of FKBP5 in the mPFC, HIP (r = 0.52, P = 0.04), Amy and HT. **(D)** SGK1 mRNA expression in the mPFC, HIP, Amy and HT (*Stress susceptibility*, $F_{(2, 13)}$ = 4.318, P = 0.0303). **(E)** Linear correlation between the arousal score and the expression of SGK1 in the mPFC, HIP, Amy and HT. **(F)** BDNF mRNA expression in the mPFC (*Stress susceptibility*, $F_{(2, 22)}$ = 4.65, P = 0.0206), HIP (*Stress susceptibility*, $F_{(2, 22)}$ = 3.50, P = 0.047), Amy (*Stress susceptibility*, $F_{(2, 13)}$ = 27.79, P < 0.0001) and HT (*Stress susceptibility*, $F_{(2, 13)}$ = 10.7, P = 0.0018). **(G)** Linear correlation between the arousal score and the expression of BDNF in the mPFC, HIP (r = 0.77, P = 0.0006), Amy (r = 0.67, P = 0.03) and HT. **(H)** NR3C1 mRNA expression in the mPFC (*Stress susceptibility*, $F_{(2, 22)}$ = 7.429, P = 0.0034), HIP, Amy (*Stress susceptibility*, $F_{(2, 13)}$ = 7.958, P = 0.0055) and HT (*Stress susceptibility*, $F_{(2, 13)}$ = 6.471, P = 0.0112). **(I)** Linear correlation between the arousal score and the expression of NR3C1 in the mPFC (r = 0.78, P = 0.0006), HIP, Amy and HT. One-way ANOVA followed by Bonferroni *post hoc* test: *p < 0.05,**P < 0.01, ***P < 0.001 vs control; #p < 0.05, ##P < 0.01, ###P < 0.001 vs susceptible. Values are expressed as means ± s. e. m. mPFC = medial prefrontal cortex; HIP = hippocampus; Amy = amygdala; HT = hypothalamus.
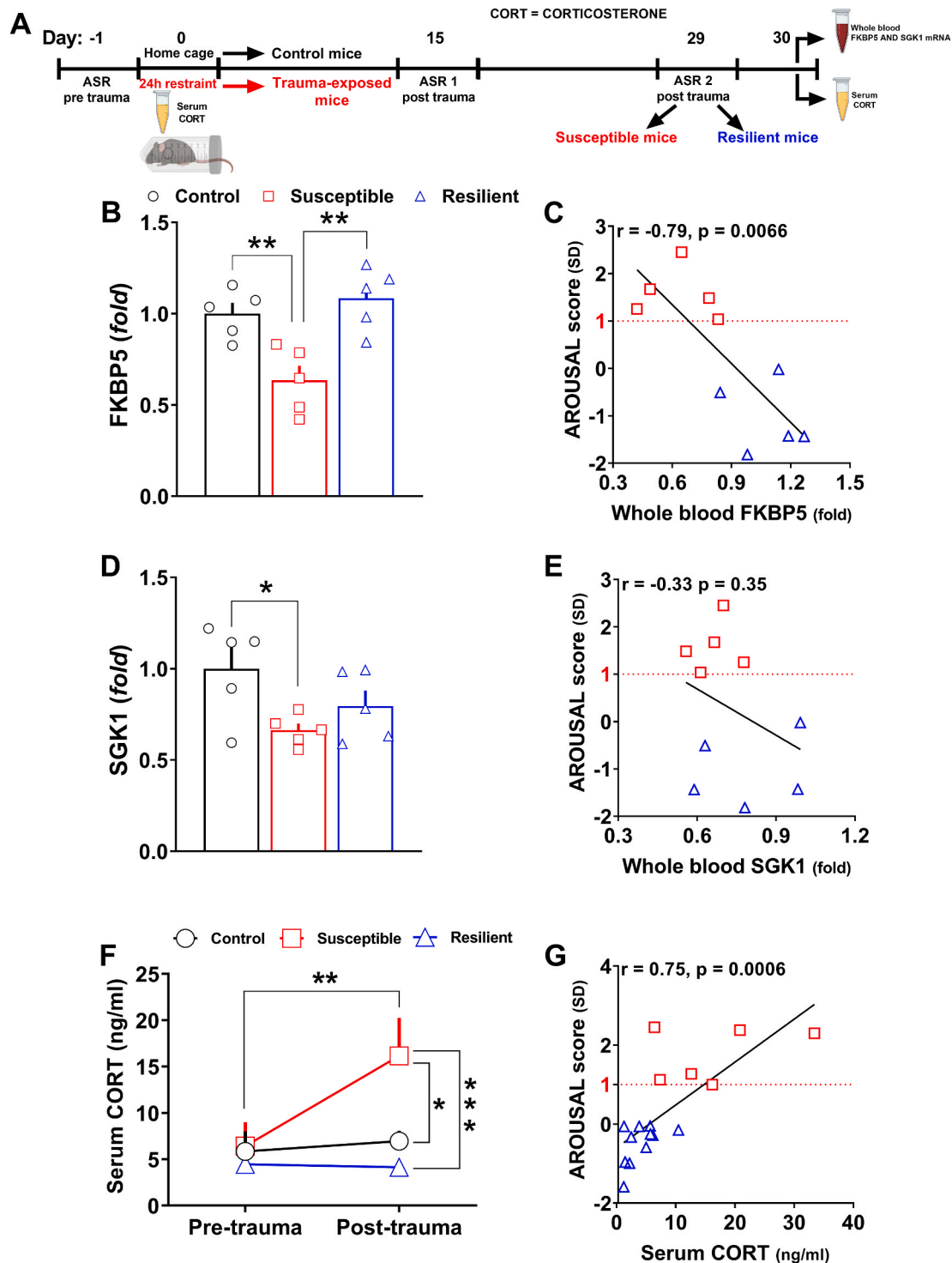
Fig. 5. *Divergent peripheral transcriptional signatures driven by selected PTSD candidate genes as well as marks of HPA axis dysfunction further validated the segregation in susceptible and resilient subpopulations.* **(A)** Timeline: the day after the segregation, control (n = 5), susceptible (n = 5) and resilient mice (n = 5) from one cohort were sacrificed to collect whole blood. Abundance of transcripts was assessed by qPCR. In other control (n = 7), susceptible (n = 6) and resilient mice (n = 11) from an independent cohort, serum was isolated from blood collected both 5–6 h before the trauma and the day after the identification in subpopulations. **(B)** FKBP5 mRNA expression (*Stress susceptibility*, $F_{(2, 12)} = 10.82$, P = 0.0021) in the whole blood. **(C)** Linear correlation between the arousal score and the expression of FKBP5 in the whole blood (r = −0.79, P = 0.0066). **(D)** SGK1 mRNA expression (*Stress susceptibility*, $F_{(2, 12)} = 3.945$, P = 0.048) in the whole blood. **(E)** Linear correlation between the arousal score and the expression of SGK1 in the whole blood. **(F)** Pre-trauma and post-trauma serum corticosterone levels (*Stress susceptibility*, $F_{(2, 21)} = 4.984$, P = 0.0169; *Time* $F_{(1, 21)} = 7.306$, P = 0.0133; *Stress susceptibility* x *Time* $F_{(2, 21)} = 5.474$, P = 0.0122). **(G)** Linear correlation between the arousal score and post-trauma serum corticosterone level (r = 0.75, P = 0.0006). Fold changes are expressed relative to transcript levels of control mice. Two-way RM ANOVA or one-way ANOVA followed by Bonferroni *post hoc* test: *P < 0.05, **P < 0.01, ***P < 0.001. Values are expressed as means ± s. e.m.
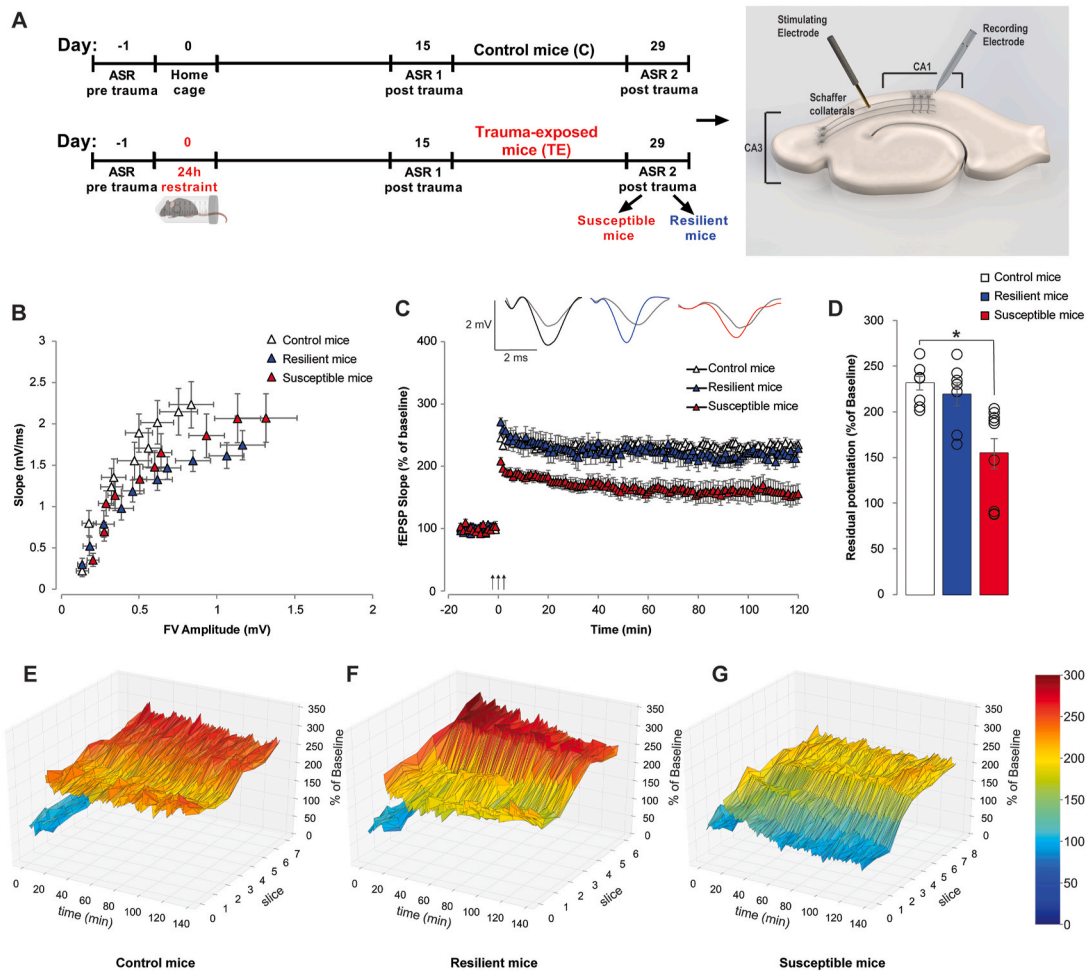
Fig. 6. *LTP is impaired only in susceptible mice identified through the AIS model.* **(A)** Experimental design. On the right, cartoon representing electrodes placement within the hippocampal slice. **(B)** No differences in fEPSP slope or fiber volley (FV) are found when analyzing Basal Synaptic Transmission (BST) in control (n = 9 slices from 6 animals), resilient (n = 9 slices from 6 animals) and susceptible mice (n = 9 slices from 7 animals). **(C)** Long-Term Potentiation (LTP) is not impaired in resilient mice (234.68 ± 7.52 vs. 228.26 ± 13.77% of baseline; n = 7/8 slices from 6/7 animals), whereas it is impaired in susceptible mice (155.94 ± 15.72% of baseline; *Stress susceptibility*, $F_{(1,13)}$ = 16.505, P = 0.001, n = 9 slices from 7 animals). On top: representative traces of recoded fEPSPs comparing baseline (light grey) and last recording point (colored). **(D)** Residual potentiation (average of the last 5 min of LTP recording at 120 min after tetanus) analysis confirms the LTP impairment in susceptible mice (*Stress susceptibility*, $F_{(2,21)}$ = 9.403, P = 0.001 among all; controls: 231.39 ± 7.35% of baseline; resilient: 218.94 ± 12.60% of baseline; susceptible: 154.41 ± 15.72% of baseline). **(E)** Triangular surface plot representing the individual traces of LTP recordings for each slice from control, **(F)** resilient, and **(G)** susceptible mice. Two-way repeated measures ANOVA or One-way ANOVA. Bonferroni *post hoc* test: *P < 0.05. Values are expressed as means ± s. e.m.

normalization provided a comprehensive view of the effects of paroxetine through the creation of the PTSD-like score. Indeed, this score altogether summarized the general beneficial effect of the pharmacological treatment in susceptible mice as well as the general detrimental effect of the same treatment in both control and resilient mice (Fig. 7L, *Treatment* $F_{(1, 37)}$ = 15.05, P = 0.0004; *Stress susceptibility* $F_{(2, 37)}$ = 14.31, P < 0.0001; *Treatment x Stress susceptibility* $F_{(2, 37)}$ = 17.45, P < 0.0001). Finally, paroxetine significantly rescued the increased mRNA expression of BDNF (Fig. S3A, *Treatment*, $F_{(2, 15)}$ = 6.93, P = 0.0074) and FKBP5 (Fig. S3B, *Treatment*, $F_{(2, 15)}$ = 4.3, P = 0.033) in the mPFC of susceptible mice.

4. Discussion

The present data indicate that the AIS model includes many key features required to shape a translational animal model for the study of PTSD. Starting from the type of trauma, the 24 h restraint stress is a single, long and severe traumatic procedure endowed with ecological validity in that a similar threatening trapping situation can happen in the natural environment of rodents (Goswami et al., 2013; Kondrakiewicz et al., 2019). This trauma may be also translationally relevant. Indeed, it would model the trapping situations experienced by survivors of natural disasters, who are at high risk of developing PTSD (Basoglu et al., 2002). With respect to the duration and severity of the trauma, a traumatic procedure of short duration should be sufficient to provoke PTSD-like phenotypes (Siegmund and Wotjak, 2006). However, C57BL6/J mice are mice generally resilient to stress and specifically resilient to single restrain stress of short duration (Flint and Tinkle, 2001; Mozhui et al., 2010). Here we show for the first time that a single severe restraint of long duration represent a traumatic procedure able to go successfully beyond the coping abilities of mice by triggering long-term and persistent PTSD-like phenotypes. This trauma was coupled to the z-normalization that firstly allowed us to capture the individual trauma susceptibility/resilience according to long-term change of startle reactivity. Startle circuits are highly conserved in connectivity and function across most species (Bale et al., 2019). Also, animals and humans are tested in a similar way. Thus, the probability of gaining translational information focusing on startle reactivity is very high. Importantly, compared to other models employing the ASR to divide animals in susceptible and resilience (Olson et al., 2011), the z-normalization had the advantage to capture the temporal fluctuation of ASR both in term of magnitude and latency at different post-trauma
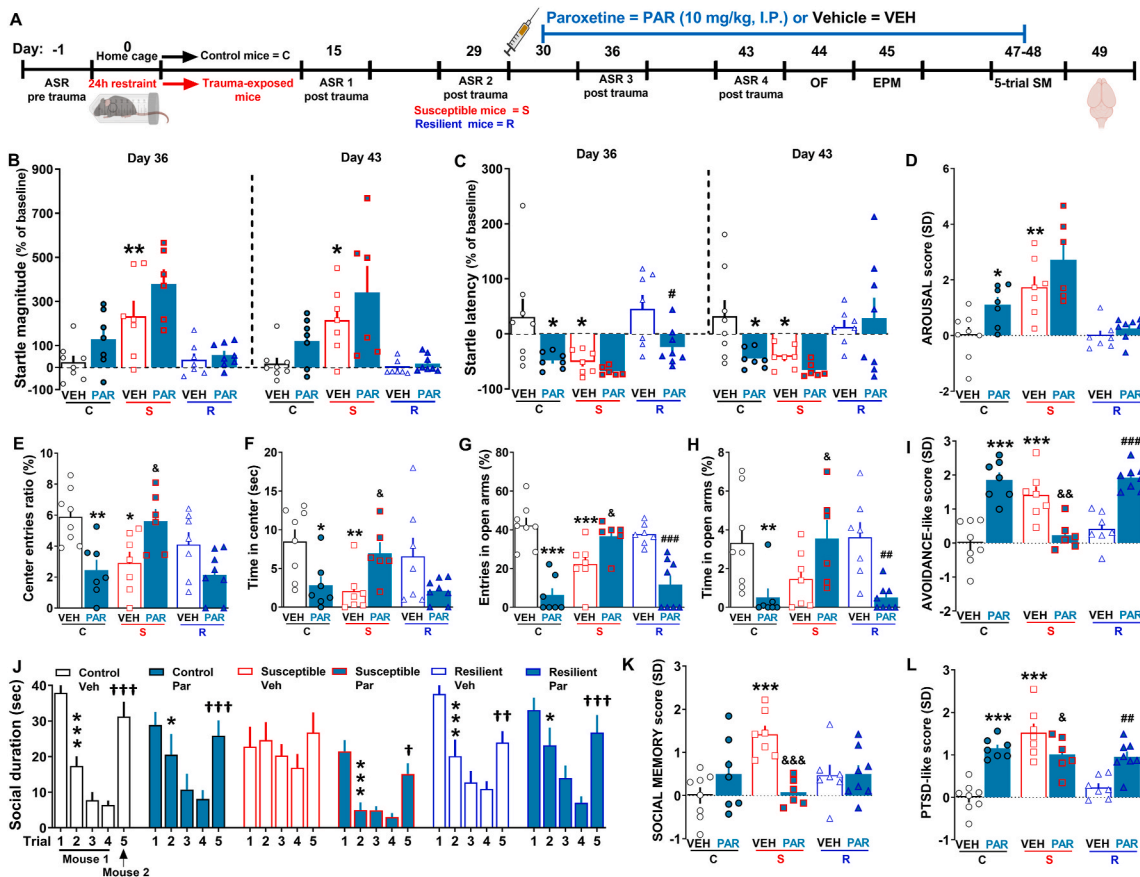
Fig. 7. *Chronic treatment with paroxetine was effective in susceptible mice but detrimental in control and resilient mice.* **(A)** Experimental timeline designed for the assessment of the effect of chronic treatment with paroxetine in control (vehicle n = 8, paroxetine n = 7), susceptible (vehicle n = 7, paroxetine n = 6) and resilient mice (vehicle n = 7, paroxetine n = 8). **(B)** Startle magnitude (% of baseline) (Day 36: *Treatment,* $F_{(1, 37)}$ = 6.024, P = 0.019; *Stress susceptibility,* $F_{(2, 37)}$ = 18.88, P < 0.0001. Day 43: *Treatment,* $F_{(1, 37)}$ = 3.84, P = 0.049; *Stress susceptibility,* $F_{(2, 37)}$ = 14.25, P < 0.0001). **(C)** Startle latency (% of baseline) (Day 36: *Treatment,* $F_{(1, 37)}$ = 12.02, P = 0.0014; *Stress susceptibility,* $F_{(2, 37)}$ = 6.64, P = 0.0034. Day 43: *Stress susceptibility,* $F_{(2, 37)}$ = 5.271, P = 0.0097). **(D)** AROUSAL score (*Treatment,* $F_{(1, 37)}$ = 8.67, P = 0.0056; *Stress susceptibility,* $F_{(2, 37)}$ = 22.23, P < 0.0001). **(E)** Center entries ratio (*Treatment x Stress susceptibility* $F_{(2, 37)}$ = 10.45, P = 0.0003) and **(F)** time spent in center of the OF (*Treatment x Stress susceptibility* $F_{(2, 37)}$ = 7.45, P = 0.0019). **(G)** Entries in open arms (*Treatment* $F_{(1, 37)}$ = 25.14, P < 0.0001; *Treatment x Stress susceptibility* $F_{(2, 37)}$ = 22.68, P < 0.0001) and **(H)** time in open arms of EPM (*Treatment* $F_{(1, 37)}$ = 5.29, P = 0.0272; *Treatment x Stress susceptibility* $F_{(2, 37)}$ = 8.77, P = 0.0008). **(I).** AVOIDANCE-like score (*Treatment* $F_{(1, 37)}$ = 18.3, P < 0.0001; *Treatment x Stress susceptibility* $F_{(2, 37)}$ = 30.48, P < 0.0001). **(J)** Social duration during the 5-trial SM test [*Treatment x trial,* $F_{(20, 144)}$ = 3.065, P < 0.0001; *Trial,* $F_{(4, 144)}$ = 74.6, P < 0.0001. Bonferroni post hoc test: *p < 0.05, ***p < 0.001 vs each specific trial 1 (habituation); †p < 0.05, ††p < 0.01, †††p < 0.001 vs each specific trial 5 (dishabituation)]. **(K)** SOCIAL MEMORY score (*Treatment x Stress susceptibility* $F_{(2, 37)}$ = 8.69, P = 0.0008). **(L)** PTSD-like score 2 (*Treatment* $F_{(1, 37)}$ = 15.05, P = 0.0004; *Stress susceptibility* $F_{(2, 37)}$ = 14.31, P < 0.0001; *Treatment x Stress susceptibility* $F_{(2, 37)}$ = 17.45, P < 0.0001). Two-way ANOVA or one-way ANOVA followed by Bonferroni *post hoc* test *P < 0.05, **P < 0.01, ***P < 0.001 vs vehicle-treated control mice, &P < 0.05, &&P < 0.01, &&&P < 0.001 vs vehicle-treated susceptible mice, #P < 0.05, ##P < 0.01, ###P < 0.001 vs vehicle-treated resilient mice. Values are expressed as means ± s. e.m.

time points. ; The discrimination between susceptible and resilient individuals seems particularly relevant given that only few PTSD preclinical studies involving mice have included this aspect (Olson et al., 2011; Sillivan et al., 2017). In fact, in numerous other studies trauma susceptibility/resilience is not reported and all comparisons are made between naive vs. trauma-exposed animals (Cohen et al., 2004; Flandreau and Toth, 2018; Goswami et al., 2013; Hendriksen et al., 2014; Richter-Levin et al., 2019; Zhang et al., 2019). Furthermore, many preclinical models are based on fear-related aspects of PTSD, whereas the AIS model cover multiple aspects listed in DSM-5 for PTSD diagnosis (American Psychiatric Association DSM-5 Task Force, 2013). Indeed, PTSD cannot be symptomatically restricted only to re-experiencing of the trauma in terms of maladaptive retention of fearful intrusive memories, and other PTSD symptoms may not be linked to dysregulated fear processes (Krystal et al., 2017). The segregation obtained through the AIS model was performed long post-trauma, consistent with PTSD diagnosis that relies on long-term symptoms, rather than on acute physiological symptoms appearing in the aftermath of the trauma

(American Psychiatric Association DSM-5 Task Force, 2013). Another important aspect of PTSD diagnosis is related to the duration of the symptoms that must last for more than one month (criterion F of DSM-5). In line with this criterion, we found that susceptible mice identified through the AIS model showed several long-lasting PTSD-like phenotypes, resembling PTSD symptoms, belonging to all criterions of DSM-5.

Of note, different than the study of Chu and colleagues (Chu et al., 2016) showing that the 24 h restraint stress produces decreased performances in mice tested in the FST, susceptible and resilient mice identified through the AIS model did not display depressive-like phenotypes. This may be due to differences in experimental settings. Despite a similar timing of experiments, both the experimental protocols and the battery behavioral tests carried out were different.

The exposure to a trauma is not sufficient to trigger PTSD. Other risk factors are involved in shaping susceptibility to develop this pathology and a useful animal model should include the study of factors predicting susceptibility/resilience to trauma/stress (Richter-Levin et al., 2019).

For instance, it has been reported that preexisting differences in social rank predicts vulnerability/resilience to chronic social defeat stress (Cherix et al., 2020; Larrieu et al., 2017). Here we found attenuated startle reactivity only in susceptible mice before the trauma. Thus, our data suggest that a pre-trauma low startle reactivity might represent a risk factor predicting the development of PTSD, and also that the AIS model is a tool that can potentially identify risk factors predicting trauma susceptibility/resilience.

We uncovered novel transcriptional signatures driven by PTSD candidate genes that supported the segregation in subpopulations and correlated with trauma susceptibility/resilience. In particular, we found an upregulation and a downregulation of FKBP5 respectively in the mPFC and whole blood of susceptible mice respectively. These findings also validate the AIS model. Indeed, they are consistent with human results showing a cortical upregulation of FKBP5 (Young et al., 2015) and a downregulation of it in the whole blood of individuals with PTSD (Yehuda et al., 2009). Such an opposite trend of FKBP5 expression in the brain and in the blood has been already reported. Whereas in the brain an upregulation of FKBP5 after GR activation may subserve the formation of trauma susceptibility mechanisms (Zannas et al., 2016), a downregulation of this gene in the blood has been associated with disrupted glucocorticoid sensitivity in blood cells (Sarapas et al., 2011; Yehuda et al., 2009). We also found a significant negative correlation between the arousal score and the expression of FKBP5 in the whole blood of mice, in line with human findings (Sarapas et al., 2011). In contrast, FKBP5 was downregulated subcortically in resilient mice in agreement with findings reporting a pro-resilience effect after inhibition of FKBP5 (Zannas et al., 2016). Regarding BDNF, whereas its role is well-established in MDD (Duman et al., 2019; Tornese et al., 2019), its role in trauma susceptibility and in trauma and stressor-related disorders such as PTSD is still unclear (Notaras and van den Buuse, 2020). Here we found an upregulation of this gene in the mPFC and HIP of susceptible mice. These results are in line with the recently proposed BDNF stress–sensitivity hypothesis, which postulates that a glucocorticoids-induced enhancement of BDNF may guide the manifestation of trauma susceptibility by promoting fear memory consolidation (Notaras and van den Buuse, 2020; Revest et al., 2014). Moreover, the upregulation of BDNF in the HIP of susceptible mice is in line with previous studies showing an increased BDNF in the hippocampus of rodents exhibiting PTSD like phenotypes (Sharma et al., 2020; Zhang et al., 2014). On the other hand, these results do not corroborate previous findings reporting a decreased BDNF mRNA/protein in mPFC and HIP of rodents tested in other preclinical models of PTSD (Ni et al., 2020; Zhao et al., 2020). One possible explanation in this case is that this increased BDNF mRNA in the mPFC might represent a not sufficient compensatory mechanism aim at counteract a blunted cortical BDNF signaling, which has been linked to maladaptive fear memory responses/fear extinction deficits (Kataoka et al., 2019). BDNF was also detected upregulated and downregulated in the HT and Amy of resilient mice respectively. To our knowledge, this is the first evidence that such a long-term divergent pattern of BDNF expression in these subcortical stress-related brain regions triggers resilience to trauma. In addition, our data showing that downregulation of BDNF in the amygdala produces a pro-resilience effect is indirectly consistent with the opposite evidence of an association between susceptibility to fear-related behavior and increased BDNF levels in the basolateral amygdala (Chou et al., 2014; Regue et al., 2019). These findings together with the other novel transcriptional signatures and correlations we found, indicate that the AIS model is a tool able to identify molecular adaptations underlying trauma susceptibility/resilience. In particular, we quantitatively unraveled more transcriptional changes in resilient mice than susceptible mice, in agreement with previous studies showing that the resilience phenomenon triggers more molecular changes than the susceptibility phenomenon (Lorsch et al., 2018). This is of high relevance because understanding the neurobiology of resilience is essential to develop novel resilience-promoting therapeutic treatments.

PTSD is commonly associated with HPA axis dysfunction and low peripheral cortisol levels (Yehuda, 2004). However, discrepancies remain in this regard with previous other studies reporting also increased (Lindauer et al., 2006) or unchanged peripheral cortisol levels in PTSD (Speer et al., 2019). We found long-term post-trauma higher basal level of serum corticosterone exclusively in susceptible mice, in agreement with recent rodent data obtained through an animal model for the study of PTSD (Sillivan et al., 2017), and more importantly in agreement with a clinical study reporting long-term higher serum cortisol levels in earthquake survivors suffering from PTSD (Song et al., 2008). These results further validate the AIS model and may also explain the long-term hippocampal CA1 LTP impairment found only in susceptible mice. Indeed, it has been reported that high level of circulating stress hormones impairs hippocampal synaptic plasticity (Popoli et al., 2011). Furthermore, an association between hippocampal structural/connectivity deficits and PTSD symptoms has been shown (Abdallah et al., 2017). These electrophysiological findings further validate the AIS model and support the hypothesis that synaptic plasticity deficits might be responsible for PTSD symptoms.

By using the AIS model, we found preclinical evidence of paroxetine efficacy in susceptible mice. To the best of our knowledge, this is the first time that the criterion of predictive validity is included in a model for the study of PTSD taking into account the validation in susceptible mice. Thus, the AIS model might represent a novel tool to identify novel pharmacological strategies for SSRI-resistant individuals with PTSD. In fact, in agreement with human data showing that hyperarousal symptoms may often persist after treatment with SSRIs (Belkin and Schwartz, 2015), here we found that paroxetine tended to worsen the hyperarousal of susceptible mice. Moreover, in line with previous findings (Huang et al., 2014), paroxetine exerted anxiolytic-like effects in susceptible mice. We further showed for the first time that paroxetine ameliorated the social memory impairment of susceptible mice assessed in the 5-trial SM test, which is a hippocampal-dependent task (Hitti and Siegelbaum, 2014). This may be explained taking into consideration that a chronic treatment with paroxetine is able to reduce the stress-induced apoptosis of hippocampal neurons (Huang et al., 2014). We also discovered that paroxetine restored the mRNA expression of BDNF and FKBP5 in the mPFC of susceptible mice, to the level of control mice. This may further explain the beneficial effect of paroxetine in susceptible mice, and is in line with a previous work showing that FKBP5 expression increases in the mPFC after fear conditioning and that lowering its expression in this area could contribute to trauma resilience (Criado-Marrero et al., 2017). Of note, paroxetine had detrimental effect in both control and resilient mice. These results further differentiated resilient mice from susceptible mice and are in agreement with previous findings. Indeed, an increased ASR has been observed in control rats chronically treated with paroxetine at the dose of 10 mg/kg (Amodeo et al., 2015). We further found that chronic treatment with paroxetine increased general avoidance-like behavior both in control and resilient mice. This effect may be linked to the evidence that specifically in control mice, the chronic blockade of serotonin transporter by paroxetine is able to produce metabolic alterations (Zha et al., 2017), which have been indeed reported to trigger avoidance-like behavior (Zemdegs et al., 2016).

Although the evaluation of sex differences was not within the scope of this study, one potential limitation of this study is related to the lack of inclusion of a relevant risk factor for PTSD, namely the sex. As in human condition, male and female rodents display different responses to stressful and traumatic procedures (Cohen and Yehuda, 2011). However, we used male mice to avoid any confounding factor related to the hormonal status of females Thus, future studies should evaluate the effectiveness of the AIS model in female mice.

In conclusion, the AIS model is a translational and comprehensive tool that may serve for studying PTSD and, more in general, trauma susceptibility/resilience. It might be beneficial for the development of new and more effective pharmacological and psychological interventions for PTSD, for which there is a major unmet need.

CRediT authorship contribution statement

Sebastiano A. Torrisi: Conceptualization, Formal analysis, Writing - original draft, conceived and designed the study, performed behavioral and pharmacological experiments, analyzed behavioral and pharmacological data, analyzed qPCR data, wrote the manuscript. **Gianluca Lavanco:** Formal analysis, performed behavioral and pharmacological experiments, analyzed behavioral and pharmacological data. **Oriana M. Maurel:** Formal analysis, performed qPCR experiments, analyzed qPCR data. **Walter Gulisano:** Formal analysis, performed electrophysiological experiments, analyzed electrophysiological data. **Samuele Laudani:** Formal analysis, performed qPCR experiments, performed ELISA assay, analyzed ELISA data, analyzed qPCR data. **Federica Geraci:** performed behavioral and pharmacological experiments. **Margherita Grasso:** performed behavioral and pharmacological experiments. **Filippo Caraci:** performed behavioral and pharmacological experiments. **Claudio Bucolo:** Supervision, performed qPCR experiments, supervised qPCR experiments. **Marco Ragusa:** performed qPCR experiments. **Francesco Papaleo:** Supervision, supervised behavioral and pharmacological experiments. **Patrizia Campolongo:** Conceptualization, Supervision, conceived and designed the study, supervised behavioral and pharmacological experiments. **Daniela Puzzo:** Formal analysis, performed electrophysiological experiments, analyzed electrophysiological data. **Filippo Drago:** Supervision, supervised behavioral and pharmacological experiments. **Salvatore Salomone:** Conceptualization, Supervision, conceived and designed the study, supervised qPCR experiments. **Gian Marco Leggio:** Conceptualization, Supervision, Writing - original draft, conceived and designed the study, supervised behavioral and pharmacological experiments, wrote the manuscript.

Acknowledgments and disclosures.

Appendix A. Supplementary data

Supplementary data related to this article can be found at https://doi.org/10.1016/j.ynstr.2020.100286.

5. Conflict of interest statement

The authors declare that they have no conflict of interest.

References

Abdallah, C.G., Wrocklage, K.M., Averill, C.L., Akiki, T., Schweinsburg, B., Roy, A., Martini, B., Southwick, S.M., Krystal, J.H., Scott, J.C., 2017. Anterior hippocampal dysconnectivity in posttraumatic stress disorder: a dimensional and multimodal approach. Transl. Psychiatry 7, e1045.

American Psychiatric Association DSM-5 Task Force, 2013. Diagnostic and Statistical Manual of Mental Disorders: DSM-5, fifth ed. American Psychiatric Association, Washington, D.C.

Amodeo, L.R., Greenfield, V.Y., Humphrey, D.E., Varela, V., Pipkin, J.A., Eaton, S.E., Johnson, J.D., Plant, C.P., Harmony, Z.R., Wang, L., Crawford, C.A., 2015. Effects of acute or repeated paroxetine and fluoxetine treatment on affective behavior in male and female adolescent rats. Psychopharmacology 232, 3515–3528.

Bale, T.L., Abel, T., Akil, H., Carlezon Jr., W.A., Moghaddam, B., Nestler, E.J., Ressler, K. J., Thompson, S.M., 2019. The critical importance of basic animal research for neuropsychiatric disorders. Neuropsychopharmacology: official publication of the American College of Neuropsychopharmacology 44, 1349–1353.

Basoglu, M., Salcioglu, E., Livanou, M., 2002. Traumatic stress responses in earthquake survivors in Turkey. J. Trauma Stress 15, 269–276.

Belkin, M.R., Schwartz, T.L., 2015. Alpha-2 receptor agonists for the treatment of posttraumatic stress disorder. Drugs Context 4, 212286.

Berardi, A., Schelling, G., Campolongo, P., 2016. The endocannabinoid system and Post Traumatic Stress Disorder (PTSD): from preclinical findings to innovative therapeutic approaches in clinical settings. Pharmacol. Res. 111, 668–678.

Berardi, A., Trezza, V., Palmery, M., Trabace, L., Cuomo, V., Campolongo, P., 2014. An updated animal model capturing both the cognitive and emotional features of post-traumatic stress disorder (PTSD). Front. Behav. Neurosci. 8, 142.

Binder, E.B., Bradley, R.G., Liu, W., Epstein, M.P., Deveau, T.C., Mercer, K.B., Tang, Y., Gillespie, C.F., Heim, C.M., Nemeroff, C.B., Schwartz, A.C., Cubells, J.F., Ressler, K. J., 2008. Association of FKBP5 polymorphisms and childhood abuse with risk of posttraumatic stress disorder symptoms in adults. Jama 299, 1291–1305.

Breen, M.S., Bierer, L.M., Daskalakis, N.P., Bader, H.N., Makotkine, I., Chattopadhyay, M., Xu, C., Buxbaum Grice, A., Tocheva, A.S., Flory, J.D., Buxbaum, J.D., Meaney, M.J., Brennand, K., Yehuda, R., 2019. Differential transcriptional response following glucocorticoid activation in cultured blood immune cells: a novel approach to PTSD biomarker development. Transl. Psychiatry 9, 201.

Bremner, J.D., Southwick, S.M., Darnell, A., Charney, D.S., 1996. Chronic PTSD in Vietnam combat veterans: course of illness and substance abuse. Am. J. Psychiatr. 153, 369–375.

Chen, L.W., Sun, D., Davis, S.L., Haswell, C.C., Dennis, E.L., Swanson, C.A., Whelan, C.D., Gutman, B., Jahanshad, N., Iglesias, J.E., Thompson, P., Mid-Atlantic, M.W., Wagner, H.R., Saemann, P., LaBar, K.S., Morey, R.A., 2018. Smaller hippocampal CA1 subfield volume in posttraumatic stress disorder. Depress. Anxiety 35, 1018–1029.

Cherix, A., Larrieu, T., Grosse, J., Rodrigues, J., McEwen, B., Nasca, C., Gruetter, R., Sandi, C., 2020. Metabolic signature in nucleus accumbens for anti-depressant-like effects of acetyl-L-carnitine. eLife 9.

Chou, D., Huang, C.C., Hsu, K.S., 2014. Brain-derived neurotrophic factor in the amygdala mediates susceptibility to fear conditioning. Exp. Neurol. 255, 19–29.

Chu, X., Zhou, Y., Hu, Z., Lou, J., Song, W., Li, J., Liang, X., Chen, C., Wang, S., Yang, B., Chen, L., Zhang, X., Song, J., Dong, Y., Chen, S., He, L., Xie, Q., Chen, X., Li, W., 2016. 24-hour-restraint stress induces long-term depressive-like phenotypes in mice. Sci. Rep. 6, 32935.

Cohen, H., Yehuda, R., 2011. Gender differences in animal models of posttraumatic stress disorder. Dis. Markers 30, 141–150.

Cohen, H., Zohar, J., Matar, M.A., Zeev, K., Loewenthal, U., Richter-Levin, G., 2004. Setting apart the affected: the use of behavioral criteria in animal models of post traumatic stress disorder. Neuropsychopharmacology: Official Publication American College of Neuropsychopharmacol 29, 1962–1970.

Cosentino, L., Vigli, D., Medici, V., Flor, H., Lucarelli, M., Fuso, A., De Filippis, B., 2019. Methyl-CpG binding protein 2 functional alterations provide vulnerability to develop behavioral and molecular features of post-traumatic stress disorder in male mice. Neuropharmacology, 107664.

Criado-Marrero, M., Morales Silva, R.J., Velazquez, B., Hernandez, A., Colon, M., Cruz, E., Soler-Cedeno, O., Porter, J.T., 2017. Dynamic expression of FKBP5 in the medial prefrontal cortex regulates resiliency to conditioned fear. Learn. Mem. 24, 145–152.

Daskalakis, N.P., Yehuda, R., Diamond, D.M., 2013. Animal models in translational studies of PTSD. Psychoneuroendocrinology 38, 1895–1911.

Deslauriers, J., Toth, M., Der-Avakian, A., Risbrough, V.B., 2018. Current status of animal models of posttraumatic stress disorder: behavioral and biological phenotypes, and future challenges in improving translation. Biol. Psychiatr. 83, 895–907.

Duman, R.S., Deyama, S., Fogaca, M.V., 2019. Role of BDNF in the pathophysiology and treatment of depression: activity-dependent effects distinguish rapid-acting antidepressants. Eur. J. Neurosci. https://doi.org/10.1111/ejn.14630. Online ahead of print.

Everitt, B.J., Giuliano, C., Belin, D., 2018. Addictive behaviour in experimental animals: prospects for translation. In: Philosophical transactions of the Royal Society of London. Series B, Biological sciences, 373.

Flandreau, E.I., Toth, M., 2018. Animal models of PTSD: a critical review. Current topics in behavioral neurosciences 38, 47–68.

Flint, M.S., Tinkle, S.S., 2001. C57BL/6 mice are resistant to acute restraint modulation of cutaneous hypersensitivity. Toxicol. Sci. 62, 250–256.

Flory, J.D., Yehuda, R., 2015. Comorbidity between post-traumatic stress disorder and major depressive disorder: alternative explanations and treatment considerations. Dialogues Clin. Neurosci. 17, 141–150.

Furini, C., Myskiw, J., Izquierdo, I., 2014. The learning of fear extinction. Neurosci. Biobehav. Rev. 47, 670–683.

Garfinkel, S.N., Abelson, J.L., King, A.P., Sripada, R.K., Wang, X., Gaines, L.M., Liberzon, I., 2014. Impaired contextual modulation of memories in PTSD: an fMRI and psychophysiological study of extinction retention and fear renewal. J. Neurosci. : the official journal of the Society for Neuroscience 34, 13435–13443.

Gerhard, D.M., Pothula, S., Liu, R.J., Wu, M., Li, X.Y., Girgenti, M.J., Taylor, S.R., Duman, C.H., Delpire, E., Picciotto, M., Wohleb, E.S., Duman, R.S., 2020. GABA interneurons are the cellular trigger for ketamine's rapid antidepressant actions. J. Clin. Invest. 130, 1336–1349.

Girgenti, M.J., Duman, R.S., 2018. Transcriptome alterations in posttraumatic stress disorder. Biol. Psychiatr. 83, 840–848.

Golde, W.T., Gollobin, P., Rodriguez, L.L., 2005. A rapid, simple, and humane method for submandibular bleeding of mice using a lancet. Lab. Anim. 34, 39–43.

Goswami, S., Rodriguez-Sierra, O., Cascardi, M., Pare, D., 2013. Animal models of post-traumatic stress disorder: face validity. Front. Neurosci. 7, 89.

Guilloux, J.P., Seney, M., Edgar, N., Sibille, E., 2011. Integrated behavioral z-scoring increases the sensitivity and reliability of behavioral phenotyping in mice: relevance to emotionality and sex. J. Neurosci. Methods 197, 21–31.

Gulisano, W., Melone, M., Ripoli, C., Tropea, M.R., Li Puma, D.D., Giunta, S., Cocco, S., Marcotulli, D., Origlia, N., Palmeri, A., Arancio, O., Conti, F., Grassi, C., Puzzo, D., 2019. Neuromodulatory action of picomolar extracellular Abeta 42 oligomers on

presynaptic and postsynaptic mechanisms underlying synaptic function and memory. J. Neurosci. : the official journal of the Society for Neuroscience 39, 5986–6000.

Hendriksen, H., Olivier, B., Oosting, R.S., 2014. From non-pharmacological treatments for post-traumatic stress disorder to novel therapeutic targets. Eur. J. Pharmacol. 732, 139–158.

Hitti, F.L., Siegelbaum, S.A., 2014. The hippocampal CA2 region is essential for social memory. Nature 508, 88–92.

Huang, Z.L., Liu, R., Bai, X.Y., Zhao, G., Song, J.K., Wu, S., Du, G.H., 2014. Protective effects of the novel adenosine derivative WS0701 in a mouse model of posttraumatic stress disorder. Acta Pharmacol. Sin. 35, 24–32.

Jacobson, L.H., Cryan, J.F., 2007. Feeling strained? Influence of genetic background on depression-related behavior in mice: a review. Behav. Genet. 37, 171–213.

Karl, A., Schaefer, M., Malta, L.S., Dorfel, D., Rohleder, N., Werner, A., 2006. A meta-analysis of structural brain abnormalities in PTSD. Neurosci. Biobehav. Rev. 30, 1004–1031.

Kataoka, T., Fuchikami, M., Nojima, S., Nagashima, N., Araki, M., Omura, J., Miyagi, T., Okamoto, Y., Morinobu, S., 2019. Combined brain-derived neurotrophic factor with extinction training alleviate impaired fear extinction in an animal model of post-traumatic stress disorder. Gene Brain Behav. 18, e12520.

Kessler, R.C., 2000. Posttraumatic stress disorder: the burden to the individual and to society. J. Clin. Psychiatr. 61 (Suppl. 5), 4–12. ; discussion 13-14.

Kessler, R.C., Sonnega, A., Bromet, E., Hughes, M., Nelson, C.B., 1995. Posttraumatic stress disorder in the national comorbidity survey. Arch. Gen. Psychiatr. 52, 1048–1060.

Kondrakiewicz, K., Kostecki, M., Szadzinska, W., Knapska, E., 2019. Ecological validity of social interaction tests in rats and mice. Gene Brain Behav. 18, e12525.

Krystal, J.H., Abdallah, C.G., Averill, L.A., Kelmendi, B., Harpaz-Rotem, I., Sanacora, G., Southwick, S.M., Duman, R.S., 2017. Synaptic loss and the pathophysiology of PTSD: implications for ketamine as a prototype novel therapeutic. Curr. Psychiatr. Rep. 19, 74.

Larrieu, T., Cherix, A., Duque, A., Rodrigues, J., Lei, H., Gruetter, R., Sandi, C., 2017. Hierarchical status predicts behavioral vulnerability and nucleus accumbens metabolic profile following chronic social defeat stress. Curr. Biol. 27, 2202–2210 e2204.

Lebow, M., Neufeld-Cohen, A., Kuperman, Y., Tsoory, M., Gil, S., Chen, A., 2012. Susceptibility to PTSD-like behavior is mediated by corticotropin-releasing factor receptor type 2 levels in the bed nucleus of the stria terminalis. J. Neurosci. : the official journal of the Society for Neuroscience 32, 6906–6916.

Leggio, G.M., Di Marco, R., Gulisano, W., D'Ascenzo, M., Torrisi, S.A., Geraci, F., Lavanco, G., Dahl, K., Giurdanella, G., Castorina, A., Aitta-Aho, T., Aceto, G., Bucolo, C., Puzzo, D., Grassi, C., Korpi, E.R., Drago, F., Salomone, S., 2019a. Dopaminergic-GABAergic interplay and alcohol binge drinking. Pharmacol. Res. 141, 384–391.

Leggio, G.M., Torrisi, S.A., Castorina, A., Platania, C.B., Impellizzeri, A.A., Fidilio, A., Caraci, F., Bucolo, C., Drago, F., Salomone, S., 2015. Dopamine D3 receptor-dependent changes in alpha 6 GABAA subunit expression in striatum modulate anxiety-like behaviour: responsiveness and tolerance to diazepam. Eur. Neuropsychopharmacol : the journal of the European College of Neuropsychopharmacology 25, 1427–1436.

Leggio, G.M., Torrisi, S.A., Mastrogiacomo, R., Mauro, D., Chisari, M., Devroye, C., Scheggia, D., Nigro, M., Geraci, F., Pintori, N., Giurdanella, G., Costa, L., Bucolo, C., Ferretti, V., Sortino, M.A., Ciranna, L., De Luca, M.A., Mereu, M., Managò, F., Salomone, S., Drago, F., Papaleo, F., 2019b. The epistatic interaction between the dopamine D3 receptor and dysbindin-1 modulates higher-order cognitive functions in mice and humans. Mol. Psychiatr. https://doi.org/10.1038/s41380-019-0511-4. Online ahead of print. PMID: 31492942.

Lian, Y., Xiao, J., Wang, Q., Ning, L., Guan, S., Ge, H., Li, F., Liu, J., 2014. The relationship between glucocorticoid receptor polymorphisms, stressful life events, social support, and post-traumatic stress disorder. BMC Psychiatr. 14, 232.

Lindauer, R.J., Olff, M., van Meijel, E.P., Carlier, I.V., Gersons, B.P., 2006. Cortisol, learning, memory, and attention in relation to smaller hippocampal volume in police officers with posttraumatic stress disorder. Biol. Psychiatr. 59, 171–177.

Lisieski, M.J., Eagle, A.L., Conti, A.C., Liberzon, I., Perrine, S.A., 2018. Single-prolonged stress: a review of two decades of progress in a rodent model of post-traumatic stress disorder. Front. Psychiatr. 9, 196.

Longenecker, R.J., Kristaponyte, I., Nelson, G.L., Young, J.W., Galazyuk, A.V., 2018. Addressing variability in the acoustic startle reflex for accurate gap detection assessment. Hear. Res. 363, 119–135.

Lopez, J.P., Fiori, L.M., Cruceanu, C., Lin, R., Labonte, B., Cates, H.M., Heller, E.A., Vialou, V., Ku, S.M., Gerald, C., Han, M.H., Foster, J., Frey, B.N., Soares, C.N., Muller, D.J., Farzan, F., Leri, F., MacQueen, G.M., Feilotter, H., Tyryshkin, K., Evans, K.R., Giacobbe, P., Blier, P., Lam, R.W., Milev, R., Parikh, S.V., Rotzinger, S., Strother, S.C., Lewis, C.M., Aitchison, K.J., Wittenberg, G.M., Mechawar, N., Nestler, E.J., Uher, R., Kennedy, S.H., Turecki, G., 2017. MicroRNAs 146a/b-5 and 425-3p and 24-3p are markers of antidepressant response and regulate MAPK/Wnt-system genes. Nat. Commun. 8, 15497.

Lorsch, Z.S., Loh, Y.E., Purushothaman, I., Walker, D.M., Parise, E.M., Salery, M., Cahill, M.E., Hodes, G.E., Pfau, M.L., Kronman, H., Hamilton, P.J., Issler, O., Labonte, B., Symonds, A.E., Zucker, M., Zhang, T.Y., Meaney, M.J., Russo, S.J., Shen, L., Bagot, R.C., Nestler, E.J., 2018. Estrogen receptor alpha drives pro-resilient transcription in mouse models of depression. Nat. Commun. 9, 1116.

Malikowska-Racia, N., Salat, K., 2019. Recent advances in the neurobiology of posttraumatic stress disorder: a review of possible mechanisms underlying an effective pharmacotherapy. Pharmacol. Res. 142, 30–49.

Mehta, D., Binder, E.B., 2012. Gene x environment vulnerability factors for PTSD: the HPA-axis. Neuropharmacology 62, 654–662.

Morena, M., Berardi, A., Peloso, A., Valeri, D., Palmery, M., Trezza, V., Schelling, G., Campolongo, P., 2017. Effects of ketamine, dexmedetomidine and propofol anesthesia on emotional memory consolidation in rats: consequences for the development of post-traumatic stress disorder. Behav. Brain Res. 329, 215–220.

Morena, M., De Castro, V., Gray, J.M., Palmery, M., Trezza, V., Roozendaal, B., Hill, M. N., Campolongo, P., 2015. Training-associated emotional arousal shapes endocannabinoid modulation of spatial memory retrieval in rats. J. Neurosci. : the official journal of the Society for Neuroscience 35, 13962–13974.

Mozhui, K., Karlsson, R.M., Kash, T.L., Ihne, J., Norcross, M., Patel, S., Farrell, M.R., Hill, E.E., Graybeal, C., Martin, K.P., Camp, M., Fitzgerald, P.J., Ciobanu, D.C., Sprengel, R., Mishina, M., Wellman, C.L., Winder, D.G., Williams, R.W., Holmes, A., 2010. Strain differences in stress responsivity are associated with divergent amygdala gene expression and glutamate-mediated neuronal excitability. J. Neurosci. : the official journal of the Society for Neuroscience 30, 5357–5367.

Musazzi, L., Tornese, P., Sala, N., Popoli, M., 2018. What acute stress protocols can tell us about PTSD and stress-related neuropsychiatric disorders. Front. Pharmacol. 9, 758.

Ni, L., Xu, Y., Dong, S., Kong, Y., Wang, H., Lu, G., Wang, Y., Li, Q., Li, C., Du, Z., Sun, H., Sun, L., 2020. The potential role of the HCN1 ion channel and BDNF-mTOR signaling pathways and synaptic transmission in the alleviation of PTSD. Transl. Psychiatry 10, 101.

Notaras, M., van den Buuse, M., 2020. Neurobiology of BDNF in fear memory, sensitivity to stress, and stress-related disorders. Mol. Psychiatr. 25, 2251–2274.

Olson, V.G., Rockett, H.R., Reh, R.K., Redila, V.A., Tran, P.M., Venkov, H.A., Defino, M. C., Hague, C., Peskind, E.R., Szot, P., Raskind, M.A., 2011. The role of norepinephrine in differential response to stress in an animal model of posttraumatic stress disorder. Biol. Psychiatr. 70, 441–448.

Pavlovsky, L., Bitan, Y., Shalev, H., Serlin, Y., Friedman, A., 2012. Stress-induced altered cholinergic-glutamatergic interactions in the mouse hippocampus. Brain Res. 1472, 99–106.

Philbert, J., Beeske, S., Belzung, C., Griebel, G., 2015. The CRF(1) receptor antagonist SSR125543 prevents stress-induced long-lasting sleep disturbances in a mouse model of PTSD: comparison with paroxetine and d-cycloserine. Behav. Brain Res. 279, 41–46.

Philbert, J., Belzung, C., Griebel, G., 2013. The CRF(1) receptor antagonist SSR125543 prevents stress-induced cognitive deficit associated with hippocampal dysfunction: comparison with paroxetine and D-cycloserine. Psychopharmacology 228, 97–107.

Popoli, M., Yan, Z., McEwen, B.S., Sanacora, G., 2011. The stressed synapse: the impact of stress and glucocorticoids on glutamate transmission. Nat. Rev. Neurosci. 13, 22–37.

Regue, M., Poilbout, C., Martin, V., Franc, B., Lanfumey, L., Mongeau, R., 2019. Increased 5-HT2C receptor editing predisposes to PTSD-like behaviors and alters BDNF and cytokines signaling. Transl. Psychiatry 9, 100.

Revest, J.M., Le Roux, A., Roullot-Lacarriere, V., Kaouane, N., Vallee, M., Kasanetz, F., Rouge-Pont, F., Tronche, F., Desmedt, A., Piazza, P.V., 2014. BDNF-TrkB signaling through Erk 1/2 MAPK phosphorylation mediates the enhancement of fear memory induced by glucocorticoids. Mol. Psychiatr. 19, 1001–1009.

Richter-Levin, G., Stork, O., Schmidt, M.V., 2019. Animal models of PTSD: a challenge to be met. Mol. Psychiatr. 24, 1135–1156.

Sarapas, C., Cai, G., Bierer, L.M., Golier, J.A., Galea, S., Ising, M., Rein, T., Schmeidler, J., Muller-Myhsok, B., Uhr, M., Holsboer, F., Buxbaum, J.D., Yehuda, R., 2011. Genetic markers for PTSD risk and resilience among survivors of the World Trade Center attacks. Dis. Markers 30, 101–110.

Savignac, H.M., Dinan, T.G., Cryan, J.F., 2011. Resistance to early-life stress in mice: effects of genetic background and stress duration. Front. Neurosci. 5, 13.

Schell, T.L., Marshall, G.N., Jaycox, L.H., 2004. All symptoms are not created equal: the prominent role of hyperarousal in the natural course of posttraumatic psychological distress. J. Abnorm. Psychol. 113, 189–197.

Shalev, A., Liberzon, I., Marmar, C., 2017. Post-traumatic stress disorder. N. Engl. J. Med. 376, 2459–2469.

Sharma, R., Sahota, P., Thakkar, M.M., 2020. Short-term sleep deprivation immediately after contextual conditioning inhibits BDNF signaling and disrupts memory consolidation in predator odor trauma mice model of PTSD. Brain Res. 1750, 147155.

Sheynin, J., Shind, C., Radell, M., Ebanks-Williams, Y., Gilbertson, M.W., Beck, K.D., Myers, C.E., 2017. Greater avoidance behavior in individuals with posttraumatic stress disorder symptoms. Stress 20, 285–293.

Siegmund, A., Wotjak, C.T., 2006. Toward an animal model of posttraumatic stress disorder. Ann. N. Y. Acad. Sci. 1071, 324–334.

Sillivan, S.E., Joseph, N.F., Jamieson, S., King, M.L., Chevere-Torres, I., Fuentes, I., Shumyatsky, G.P., Brantley, A.F., Rumbaugh, G., Miller, C.A., 2017. Susceptibility and resilience to posttraumatic stress disorder-like behaviors in inbred mice. Biol. Psychiatr. 82, 924–933.

Smith, S.M., Vale, W.W., 2006. The role of the hypothalamic-pituitary-adrenal axis in neuroendocrine responses to stress. Dialogues Clin. Neurosci. 8, 383–395.

Smoller, J.W., 2016. The genetics of stress-related disorders: PTSD, depression, and anxiety disorders. Neuropsychopharmacology: official publication of the American College of Neuropsychopharmacology 41, 297–319.

Song, Y., Zhou, D., Wang, X., 2008. Increased serum cortisol and growth hormone levels in earthquake survivors with PTSD or subclinical PTSD. Psychoneuroendocrinology 33, 1155–1159.

Speer, K.E., Semple, S., Naumovski, N., D'Cunha, N.M., McKune, A.J., 2019. HPA axis function and diurnal cortisol in post-traumatic stress disorder: a systematic review. Neurobiology of stress 11, 100180.

Stevens, J.S., Jovanovic, T., 2019. Role of social cognition in post-traumatic stress disorder: a review and meta-analysis. Gene Brain Behav. 18, e12518.

Tornese, P., Sala, N., Bonini, D., Bonifacino, T., La Via, L., Milanese, M., Treccani, G., Seguini, M., Ieraci, A., Mingardi, J., Nyengaard, J.R., Calza, S., Bonanno, G., Wegener, G., Barbon, A., Popoli, M., Musazzi, L., 2019. Chronic mild stress induces anhedonic behavior and changes in glutamate release, BDNF trafficking and dendrite morphology only in stress vulnerable rats. The rapid restorative action of ketamine. Neurobiology of stress 10, 100160.

Torrisi, S.A., Leggio, G.M., Drago, F., Salomone, S., 2019. Therapeutic challenges of post-traumatic stress disorder: focus on the dopaminergic system. Front. Pharmacol. 10, 404.

Torrisi, S.A., Salomone, S., Geraci, F., Caraci, F., Bucolo, C., Drago, F., Leggio, G.M., 2017. Buspirone counteracts MK-801-induced schizophrenia-like phenotypes through dopamine D3 receptor blockade. Front. Pharmacol. 8, 710.

Tovote, P., Fadok, J.P., Luthi, A., 2015. Neuronal circuits for fear and anxiety. Nat. Rev. Neurosci. 16, 317–331.

Yehuda, R., 2004. Risk and resilience in posttraumatic stress disorder. J. Clin. Psychiatr. 65 (Suppl. 1), 29–36.

Yehuda, R., Cai, G., Golier, J.A., Sarapas, C., Galea, S., Ising, M., Rein, T., Schmeidler, J., Muller-Myhsok, B., Holsboer, F., Buxbaum, J.D., 2009. Gene expression patterns associated with posttraumatic stress disorder following exposure to the World Trade Center attacks. Biol. Psychiatr. 66, 708–711.

Young, K.A., Thompson, P.M., Cruz, D.A., Williamson, D.E., Selemon, L.D., 2015. BA11 FKBP5 expression levels correlate with dendritic spine density in postmortem PTSD and controls. Neurobiology of stress 2, 67–72.

Zannas, A.S., Wiechmann, T., Gassen, N.C., Binder, E.B., 2016. Gene-stress-epigenetic regulation of FKBP5: clinical and translational implications. Neuropsychopharmacology : official publication of the American College of Neuropsychopharmacology 41, 261–274.

Zapala, M.A., Hovatta, I., Ellison, J.A., Wodicka, L., Del Rio, J.A., Tennant, R., Tynan, W., Broide, R.S., Helton, R., Stoveken, B.S., Winrow, C., Lockhart, D.J., Reilly, J.F., Young, W.G., Bloom, F.E., Lockhart, D.J., Barlow, C., 2005. Adult mouse brain gene expression patterns bear an embryologic imprint. Proc. Natl. Acad. Sci. U.S.A. 102, 10357–10362.

Zemdegs, J., Quesseveur, G., Jarriault, D., Penicaud, L., Fioramonti, X., Guiard, B.P., 2016. High-fat diet-induced metabolic disorders impairs 5-HT function and anxiety-like behavior in mice. Br. J. Pharmacol. 173, 2095–2110.

Zha, W., Ho, H.T.B., Hu, T., Hebert, M.F., Wang, J., 2017. Serotonin transporter deficiency drives estrogen-dependent obesity and glucose intolerance. Sci. Rep. 7, 1137.

Zhang, L., Benedek, D.M., Fullerton, C.S., Forsten, R.D., Naifeh, J.A., Li, X.X., Hu, X.Z., Li, H., Jia, M., Xing, G.Q., Benevides, K.N., Ursano, R.J., 2014. PTSD risk is associated with BDNF Val66Met and BDNF overexpression. Mol. Psychiatr. 19, 8–10.

Zhang, L., Hu, X.Z., Li, H., Li, X., Yu, T., Dohl, J., Ursano, R.J., 2019. Updates in PTSD animal models characterization. Methods Mol. Biol. 2011, 331–344.

Zhao, M., Wang, W., Jiang, Z., Zhu, Z., Liu, D., Pan, F., 2020. Long-term effect of post-traumatic stress in adolescence on dendrite development and H3K9me2/BDNF expression in male rat Hippocampus and prefrontal cortex. Front Cell Dev Biol 8, 682.